5-Hydroxyindole-2-carboxylic Acid Amides: Novel Histamine-3 Receptor Inverse Agonists for the Treatment of Obesity

Pascale David Pierson, Alec Fettes, Christian Freichel, Silvia Gatti-McArthur, Cornelia Hertel, Jörg Huwyler, Peter Mohr, Toshito Nakagawa, Matthias Nettekoven, Jean-Marc Plancher,* Susanne Raab, Hans Richter, Olivier Roche, Rosa María Rodríguez Sarmiento, Monique Schmitt, Franz Schuler, Tadakatsu Takahashi, Sven Taylor, Christoph Ullmer, and Ruby Wiegand

F. Hoffmann-La Roche Ltd., Pharmaceuticals Division, CH-4070 Basel, Switzerland

Received February 6, 2009

Obesity is a major risk factor in the development of conditions such as hypertension, hyperglycemia, dyslipidemia, coronary artery disease, and cancer. Several pieces of evidence across different species, including primates, underscore the implication of the histamine 3 receptor (H_3R) in the regulation of food intake and body weight and the potential therapeutic effect of H_3R inverse agonists. A pharmacophore model, based on public information and validated by previous investigations, was used to design several potential scaffolds. Out of these scaffolds, the 5-hydroxyindole-2-carboxylic acid amide appeared to be of great potential as a novel series of H_3R inverse agonist. Extensive structure−activity relationships revealed the interconnectivity of microsomal clearance and hERG (human ether-a-go-go-related gene) affinity with lipophilicity, artificial membrane permeation, and basicity. This effort led to the identification of compounds reversing the (*R*)-α-methylhistamine-induced water intake increase in Wistar rats and, further, reducing food intake in diet-induced obese Sprague−Dawley rats. Of these, the biochemical, pharmacokinetic, and pharmacodynamic characteristics of (4,4-difluoropiperidin-1-yl)[1-isopropyl-5-(1-isopropylpiperidin-4-yloxy)-1*H*-indol-2-yl]-methanone **36** are detailed.

Introduction

In the past 2 decades, obesity has became epidemic and is nowadays recognized as a significant health care burden. Already in 1997, the World Health Organisation (WHO[a]) officially declared human obesity as one of the most significant health problems facing mankind.[1] This declaration followed the massive expansion in the prevalence of obesity in almost all societies.[2a,3a] According to the WHO body mass index (BMI) classification, more than 120 million people are today considered obese. Obesity is a major risk factor for the development of conditions such as hypertension, hyperglycemia, dyslipidemia, coronary artery disease, and cancer.[3,4] As a consequence, the total cost in the U.S. for all obesity-related health problems exceeds $200 billion. Sadly, 400 000 people die each year prematurely in the U.S. from obesity-related complications.[5] Increasingly sedentary lifestyles and high-fat, energy rich diets are the two main causes for the global rise in the prevalence of obesity. Several drugs have reached the market, among them the most prominent being sibutramine (a nonselective norepinephrine/serotonine/dopamine reuptake inhibitor) and orlistat (a lipase inhibitor).[2] The obesity market is expected to increase to over U.S. $1.3 billion by 2010.[6] However, their potential side effects, the perception the patient has of his own disease, and additionally the discrepancy between the patient's expectation and the achievable weight loss under medication (typically 5% within 1 year) are hampering compliance.[7] Although a change of lifestyle remains an excellent therapy, there exists a large medical need for safe and efficient treatment of obesity, stimulating research in this field.[2]

Histamine 3 Receptor Subtype and Its Pharmacology. Belonging to the G-protein-coupled receptor (GPCR) type A superfamily, the histamine receptor family consists of four subtypes.[8] The histamine H_1 and H_2 receptors (H_1R and H_2R) have already been extensively studied, particularly for their involvement in the modulation of allergic response and gastric acid secretion, respectively, leading to the identification of very useful medicines.[9] The H_4 receptor (H_4R) was discovered more recently,[10,11] and its potential utility is still being investigated.[12]

The histamine 3 receptor (H_3R), discovered in 1983,[13] cloned in 1999 (human receptor),[14] and consisting of 445 amino acids, shares limited similarity with its H_1R, H_2R, and H_4R congeners and is predominantly expressed in the central nervous system (CNS). As a presynaptic autoreceptor, H_3R is negatively coupled to adenylcyclase and regulate neurotransmitter releases. Its blockade increases the synthesis and the release of histamine,[13] which in turn can bind to and activate central H_1R. It has been proposed that stimulation of H_1R can reduce food intake and increase wakefulness.[15,16d] H_3R has also been shown to act as a heteroreceptor, regulating the release of other neurotransmitters such as acetylcholine, dopamine, norepinephrine, and serotonin,[16d] known for their important roles in modulating vigilance, attention, and cognitive function.

The H_3R is a constitutively active receptor,[17] and ligands have been described as falling into three functional classes: agonists, inverse agonists, and neutral antagonists.

* To whom correspondence should be addressed. Phone: +41 61 68 86 725. Fax: +41 61 68 88 714. E-mail: jean-marc.plancher@roche.com.

[a] Abbreviations: aq, aqueous; b.i.d., bis in die (twice a day); BMI, body mass index; BSS, behavioral satiety sequence; CNS, central nervous system; DCM, dichloromethane; DIO, diet induced obesity; h, human; DMF, *N*,*N*-dimethylformamide; H_1R, histamine-1 receptor subtype; H_2R, histamine-2 receptor subtype; H_3R, histamine-3 receptor subtype; H_4R, histamine-4 receptor subtype; hERG, human ether-a-go-go-related gene; HFD, high-fat diet; HPLC, high pressure liquid chromatography; ip, intraperitonal; LYSA, lyophilization solubility assay; MNT, micrometerucleus test; OGTT, oral glucose tolerance test; po, per os (oral); RAMH, (*R*)-α-methylhistamine; SD, Sprague−Dawley; TBTU, 2-(1*H*-benzotriazole-1-yl)-1,1,3,3-tetramethyluronium tetrafluoroborate; THF, tetrahydrofuran; U.S., United States of America; WHO, World Health Organization.

10.1021/jm900409x CCC: $40.75
Published on Web 05/20/2009

Scheme 1. Some Representative H_3R Antagonists/Inverse Agonists: **1**−**6** Used as Preclinical Tools and **7**−**9** Claimed To Be in Clinical Trials[a]

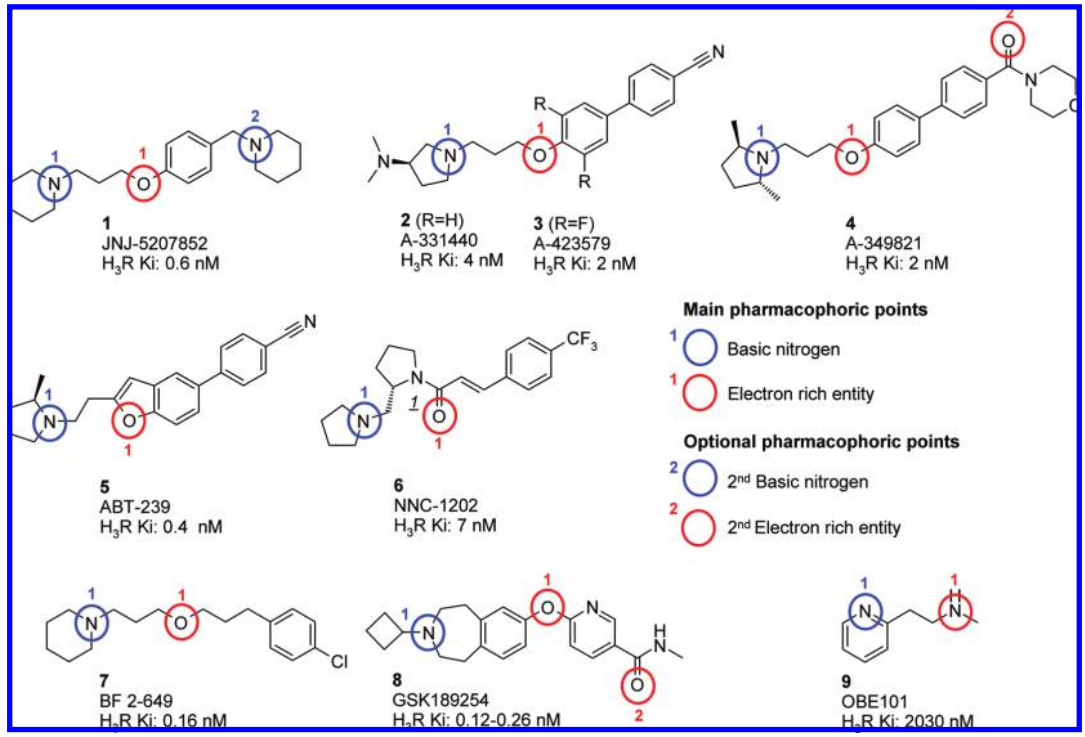

[a] Colored circles highlight the conserved pharmacophore requirements.

Over 20 isoforms of the human H_3R have been identified so far, varying in length, N and C termini, sequence of the third intracellular loop, and deletions of transmembrane domains, although pharmacological relevance of these isoforms remain elusive.[18]

As a consequence of this complex and rich pharmacology, H_3R antagonists/inverse agonists are raising interest in two main fields: cognitive diseases/sleep disorders[16,19] (e.g., Alzheimer, depression, anxiety, schizophrenia, and narcolepsy) and metabolic diseases (e.g., obesity, dyslipidemia).[16,20]

Historically, the first H_3R antagonists/inverse agonists were derived directly from the endogenous ligand histamine and therefore contained the imidazole core. This pharmacophore was perceived to be responsible for two majors drawbacks, namely, significant binding discrepancies across species (e.g., rat vs human H_3R binding properties)[21] and undesired affinity for the cytochromes P450.[22] A breakthrough came with the replacement of the offending imidazole by a tertiary amine. Several nonimidazole-based compounds unleashed the rich H_3R pharmacology in both the cognition/sleep and food intake arenas but revealed also some of the undesired properties and limitations linked to the H_3R pharmacophore or its different chemical series (see Scheme 1).[23] Representative of the innovative piperidine-3-propyloxy motif, **1** (JNJ-5207852) is flanked by a second basic nitrogen.[24] **1** is a tight and selective H_3R binder with clear in vivo efficacy in rodent arousal models and interestingly lacks the appetite-suppressant effect.[24]

Capitalizing as well on the propyloxy motif, **2** (A-331440) demonstrates sustained efficacy in chronic obesity models, mainly by reducing adipose tissues mass, and a modest effect in the cognition enhancing model.[25,26] However, **2** was reported to be genotoxic in the in vitro micronucleus test (MNT).[27] Fortunately, some of its fluorinated congeners, e.g., **3** (A-423579), were devoid of any in vitro genotoxicity while retaining efficacy in obesity models.[27] Another aminopropyloxybiphenyl, **4** (A-349821), was very potent in rodent model of cognitive enhancement, yet did not show any effect in an obesity model, even at higher dose.[23,28] This distinct pharmacology between obesity and cognitive/arousal models, also reported above for **1**, remains to be explained.[26] Eventually, development of **4** was terminated because of an inadequate safety margin with respect to a prolonged duration of cardiac action potential.[23] **5** (ABT-239)[29] showed broad efficacy in preclinical models of cognitive deficits;[29c] however, its safety ratio toward cardiovascular risk was not sufficient for development, despite a more favorable brain/blood ratio compared to **4**.[30] Again, **5** was claimed to be ineffective in a rodent model of obesity (at 30 mg/kg).[26] Finally, **6** (NNC-1202) brings an additional piece of evidence by successfully reducing average calorie intake in rhesus monkeys.[31] However, neither application of this compound in cognitive models nor any clinical developments have been reported.

Three representatives compounds currently in clinical trials are listed in Scheme 1, two of which are being evaluated in phase II for narcolepsy (**7**, BF 2.649;[32] **8**, GSK189254[33]). Interestingly, only **9** (OBE101), which has already been marketed to treat vestibular vertigo, went successfully into phase II with obesity as indication.[34] Surprisingly, affinity of **9** for the rat H_3R was reported to be only in the micromolar range[35] (see Scheme 1). To the best of our knowledge, up to 10 H_3R antagonists/inverse agonists were tested in clinical trials.[36]

Chemistry

Prior to the synthesis of the H_3R ligands, we describe here first the preparation of some noncommercially available piperidine and piperazine derivatives.

Piperidines **12** and **15** were prepared by a double Michael addition on ethyl acrylate, followed by a Dieckmann condensation and subsequent decarboxylation and reduction of the ketone

Scheme 2. Preparation of 1-Cyclopropyl- and 1-*tert*-Butylpiperidin-4-ol **12** and **15** and 1-Cyclobutylpiperazine **17**[a]

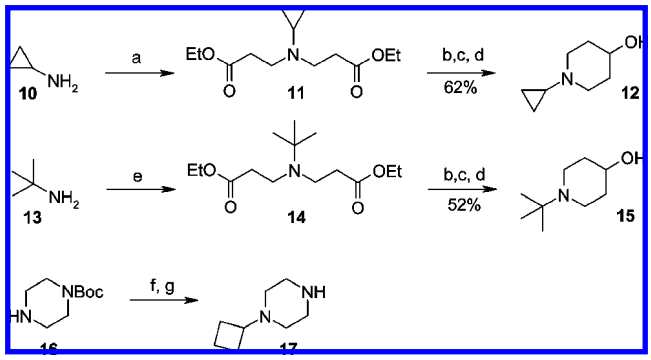

[a] Reagents and conditions: (a) ethyl acrylate 2.0 equiv, room temp, 4 days, 54%; (b) NaH 1.5 equiv, ethanol 1.0 equiv, THF, reflux, 2 days; (c) aq HCl 18%, reflux, 5 h, then NaOH 1 N; (d) $NaBH_4$ 0.75 equiv, ethanol, room temp, then aq NaOH 28%; (e) ethyl acrylate 3.5 equiv, reflux, 6 days, 14%; (f) cyclobutanone 1.0 equiv, sodium triacetoxy borohydride 1.0 equiv, DCM, room temp, 16 h, 97%; (g) 4 M HCl in dioxane, room temp, 16 h, 96%.

(see Scheme 2).[37] Steric bulk of the *tert*-butylamine dramatically decreases the reactivity of the mono-Michael adduct, leading to a modest yield despite a prolonged reaction time (14%, 6 days). *N*-Cyclobutylpiperidine **17** was prepared by reductive amination followed by acidic cleavage of the carbamate protecting group.

To facilitate the SAR exploration of the indole ring, several syntheses were developed, most of them from commercially available 2,5-disubstituted indoles. Incorporation of the morpholine into the 5-hydroxyindole-2-carboxylic acid, followed by a Mitsunobu reaction to vary the 5-substituent, proved to be the most expeditious approach, although the yields of the Mitsunobu reaction suffered from using standardized, unoptimized reaction conditions (see Scheme 3).

The use of 5- and 6-hydroxy-1*H*-indole-2-carboxylic acid ethyl esters allowed the exploration of the amide functionality (see Scheme 4). Whereas the former building block is commercially available, the 6-hydroxy isomer was prepared according to a known procedure.[38]

Derivatization of the indole nitrogen was achieved mainly by stoichiometric deprotonation using sodium hydride, followed by quenching with the appropriate electrophile (see Scheme 5, compounds **33**−**40**). An Ullmann coupling was instrumental for the incorporation of an *N*-aryl substituent (**41**).[39]

Since the 2,2,2-trifluoroethyl substituent on the indole nitrogen was found to be of particular interest, the reaction sequence was altered to allow for a late stage derivatization of the amide moiety. The Mitsunobu/N-alkylation/amidation sequence turned out to be favorable as far as the overall yield was concerned (see Scheme 6).

Introduction of the piperidine, protected as its carbamate, allowed the late modulation of the *N*-piperidine substituent (see Scheme 6). Whereas both cyclobutanone and oxetanone are commercially available and readily undergo reductive amination, leading to compounds **45** and **46**, respectively, cyclopropanone

Scheme 3. Preparation of Disubstituted Indoles from 5-Hydroxyindole-2-carboxylic Acid[a]

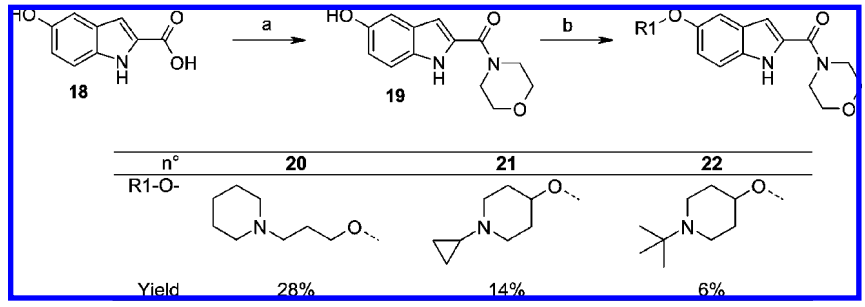

[a] Reagents and conditions: (a) morpholine 1.15 equiv, TBTU 1.15 equiv, *i*-Pr_2NEt 5.0 equiv, DMF, room temp, 16 h, 86%; (b) R1OH 1.3 equiv, azodicarbonyldipiperidine 2.0 equiv, tri-*n*-butylphosphine 2.0 equiv, THF, 0 °C to room temp, 16 h.

Scheme 4. Exploration of the 2,5- and 2,6-Positions[a]

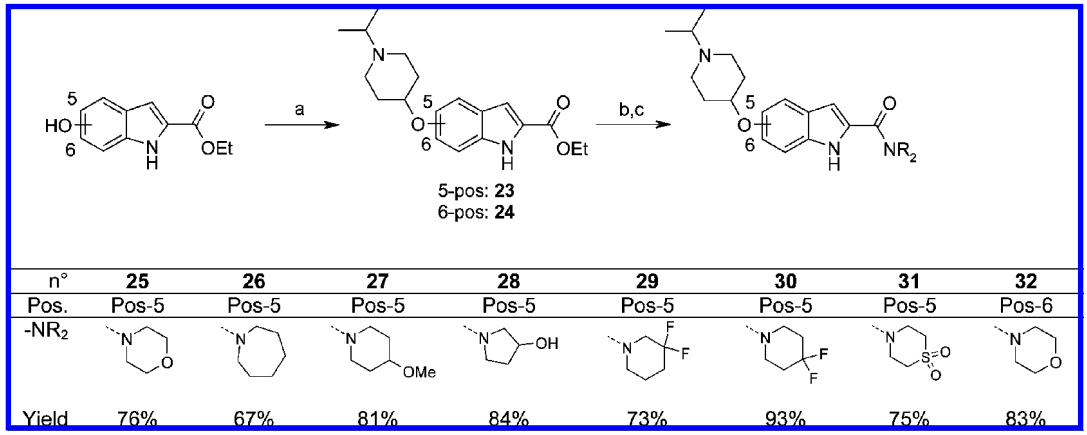

[a] Reagents and conditions: (a) 1-isopropylpiperidin-4-ol 1.2 equiv, triphenylphosphine 1.2 equiv, di-*tert*-butylazodicarboxylate 1.2 equiv, THF, room temp, 2 days, 67% (pos-5) 14% (pos-6); (b) $LiOH \cdot H_2O$ 1.1 equiv, methanol, THF, water; quant (pos-5), 99% (pos-6); (c) HNR_2 1.2 equiv, TBTU 1.2 equiv, *i*-Pr_2NEt 6.0 equiv, DMF, room temp, 16 h.

Scheme 5. Exploration of the *N*-Indole Substituent[a]

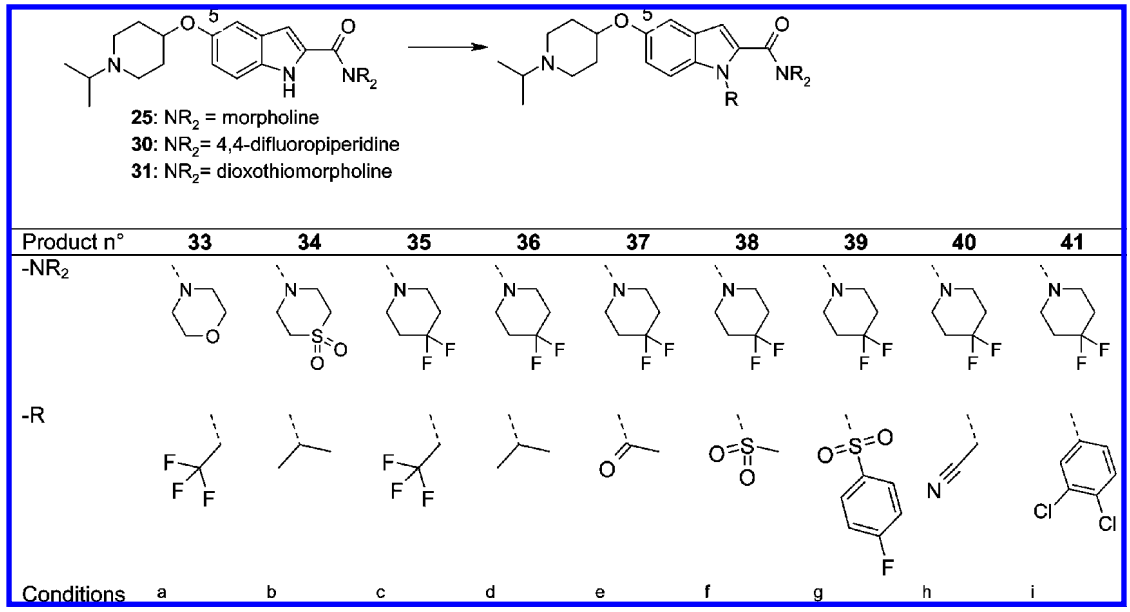

[a] Reagents and conditions: (a) **25**, 2,2,2-trifluoroethyl trifluoromethanesulfonate 1.2 equiv, NaH 1.2 equiv, DMF, 70 °C, 24 h, 74%; (b) **31**, isopropyl methanesulfonate 2.0 equiv, cesium carbonate 2.0 equiv, acetonitrile, 95 °C, 22 h, 47%; (c) **30**, 2,2,2-trifluoroethyl trifluoromethanesulfonate 1.2 equiv, NaH 1.2 equiv, DMF, 70°C, 24 h, 88%; (d) **30**, 2-bromopropane 1.1 equiv, NaH 1.2 equiv, DMF, 70 °C, 18 h, 59%; (e) **30**, acetyl chloride 2.5 equiv, NaH 1.2 equiv, DMF, room temp, 24 h, 77%; (f) **30**, methanesulfonoyl chloride 2.5 equiv, sodium hydride 1.2 equiv, DMF, room temp, 2 days, 9%; (g) **30**, 4-fluorobenzenesulfonyl chloride 1.2 equiv, NaH 1.1 equiv, DMF, 60 °C, 20 h, 60%; (h) **30**, bromoacetonitrile 1.1 equiv, NaH 1.1 equiv, DMF, 70 °C, 5 h, 38%; (i) **30**, 3,4-dichlorophenylboronic acid 3.0 equiv, copper acetate 2.0 equiv, pyridine 4.0 equiv, DCM, room temp, 3 days, 81%.

Scheme 6. Early Stage Incorporation of the 2,2,2-Trifluoroethyl Residue on the Indole Nitrogen and Variation of the *N*-Piperidine Substituent[a]

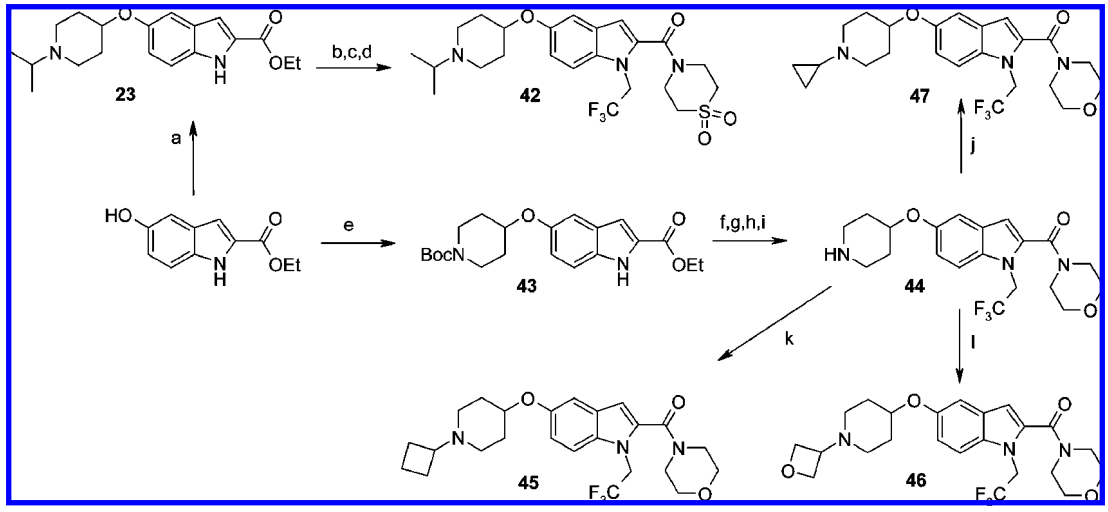

[a] (a) 1-Isopropylpiperidin-4-ol 1.2 equiv, triphenylphosphine 1.2 equiv, di-*tert*-butylazodicarboxylate 1.2 equiv, THF, room temp, 2 days, 67%; (b) 2,2,2-trifluoroethyl trifluoromethanesulfonate 1.2 equiv, NaH 1.1 equiv, DMF, 70 °C, 16 h, quant; (c) LiOH·H_2O 1.2 equiv, THF, water, methanol, reflux, 16 h, quant.; (d) dioxothiomorpholine 1.2 equiv, TBTU 1.2 equiv, *i*-Pr_2NEt 5.0 equiv, DMF, room temp, 24 h, 92%; (e) *N*-Boc-4-hydroxypiperidine 1.04 equiv, PPh_3 1.25 equiv, diisopropylazodicarboxylate 1.22 equiv, DCM, room temp, 3 days, 58%; (f) LiOH·H_2O 1.1 equiv, THF, MeOH, water, 80 °C, 16 h, 96%; (g) morpholine 1.5 equiv, *t*-BuCOCl 1.2 equiv, 4-methylmorpholine 1.2 equiv, 0 °C, 4.5 h, 75%; (h) 2,2,2-trifluoroethyl trifluoromethanesulfonate 1.2 equiv, NaH 1.1 equiv, DMF, 70°C, 20 h, 65%; (i) trifluoroacetic acid 10 equiv, DCM, room temp, 1 h, 92%; (j) (1-ethoxycyclopropoxy)trimethylsilane 1.5 equiv, sodium cyanoborohydride 1.5 equiv, acetic acid 3.0 equiv, THF, 55 °C, 20 h, 45%; (k) oxetanone 2.0 equiv, sodium triacetoxyborohydride 2.0 equiv, acetic acid 3.0 equiv, THF, 65°C, 2 h, 60%; (l) cyclobutanone 1.5 equiv, sodium cyanoborohydride 1.5 equiv, acetic acid 3.0 equiv, THF, 55 °C, 16 h, 59%.

is not available because of its large preference for the sp^3 hybridization state. However, the problem was circumvented by the use of the known (1-ethoxycyclopropyl)trimethylsilane as synthetic equivalent.[40]

5-Aminoindoles were derived from the commercially available 5-nitroindolecarboxylic acid ethyl ester (see Scheme 7). Reduction of the nitro group using hydrogen over platinium oxide did not interfere with the indole nucleus, and the piperidinyl group was introduced using a reductive amination. After the incorporation of the amide moiety, the aniline was selectively alkylated, leading to compound **50**.

The Fisher indole synthesis[41] was found to be a convenient strategy to introduce from the beginning a carboxylic acid functionality at the 5-position, later converted to the *N*-cyclobutylpiperidine amide (see Scheme 8). The 1- and 2-positions of the indole could subsequently be further manipulated.

Scheme 7. Modulation of the *N*-Piperidine Substituent[a]

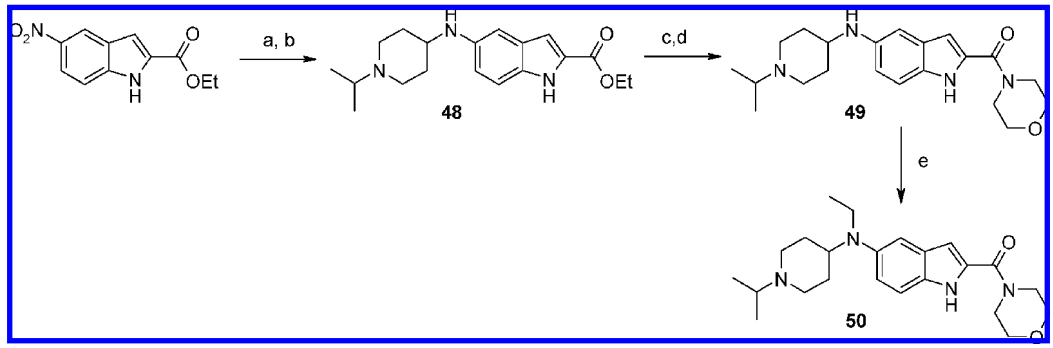

[a] (a) $PtO_2 \cdot H_2O$ 0.11 equiv, H_2, THF, room temp, 2 h, 98%; (b) 1-isopropyl-4-piperidone 1.0 equiv, Ti(O-*i*-Pr)$_4$ 1.2 equiv, $NaBH_4$ 0.6 equiv, methanol, room temp, 16 h, 85%; (c) $LiOH \cdot H_2O$ 1.1 equiv, THF, methanol, water, 75 °C, 2 h, quant; (d) morpholine 1.2 equiv, TBTU 1.2 equiv, *i*-Pr_2NEt 6.0 equiv, DMF, room temp, 2 h, 78%; (e) potassium carbonate 1.25 equiv, iodoethane 2.5 equiv, dimethylacetamide, 60 °C, 2 h, 77%.

Scheme 8. Fisher Indole Synthesis for the Preparation of 2,5-Bis-aminocarbonylindoles[a]

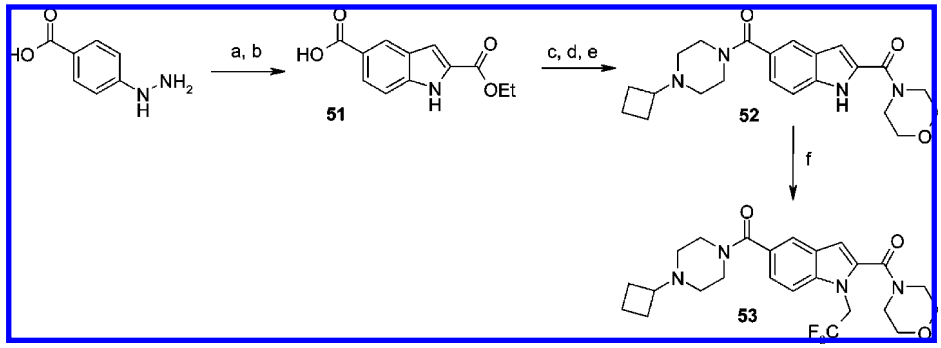

[a] (a) Ethyl pyruvate 1.2 equiv, ethanol, reflux, 18 h, 82%; (b) polyphosphoric acid, 165 °C, 20 min, 44%; (c) **17** 1.25 equiv, TBTU 1.5 equiv, *i*-Pr_2NEt, DMF, room temp, 1.5 h, 63%; (d) LiOH 1.25 equiv, THF, water, 75 °C, 2 h, quant; (e) morpholine 1.25 equiv, *i*-Pr_2NEt 5.0 equiv, TBTU 1.25 equiv, DMF, room temp, 3.5 h, 73%; (f) 2,2,2,-trifluoroethyl-trifluoromethanesulfonate 1.1 equiv, NaH 1.1 equiv, THF, 75 °C, 2 days, 76%.

Scheme 9. Preparation of 5-Hydroxy-3-carboxamideindole[a]

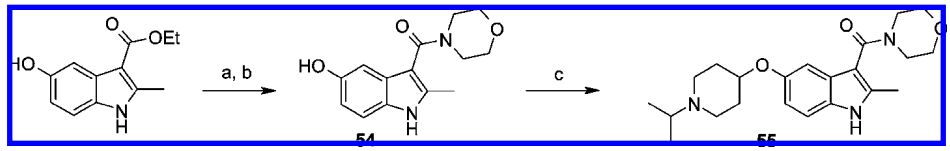

[a] (a) NaOH 5.0 equiv, THF, water, reflux, 2 days, 75%; (b) morpholine 1.2 equiv, TBTU 1.2 equiv, *i*-Pr_2NEt 5.0 equiv, DMF, room temp, 2 h, 20%; (c) 1-isopropylpiperidin-4-ol 1.3 equiv, azodicarbonyldipiperidine 2.0 equiv, tri-*n*-butylphosphine 2.0 equiv, THF, room temp, 3 days, 22%.

To explore the indole scaffold systematically, the 3,5- and 2,6-disubstituted indoles were also prepared and evaluated, in addition to the favorable 2,5-disubstituted and 1,2,5-trisubstituted derivatives. The 3,5-derivatives were assembled in a straightforward manner by saponification[42] of the commercially available ethyl 5-hydroxy-2-methylindole-3-carboxylate and subsequent standard amidation/Mitsunobu process (see Scheme 9).

Because of the lack of useful commercially available materials, the 2,6-disubstituted indoles were accessed by the Hemtsberger−Knittel reaction[41] between ethyl azidoacetate and 4-benzyloxy-3-fluorobenzaldehyde, which led mainly to the desired regioisomer **56** (see Scheme 10). Again, the electron-rich indole double bond proved to be quite stable toward hydrogenation, making the benzyl cleavage a high yield process.

Results and Discussion

Lead Identification. The publication of dozens of potent H_3R binders has facilitated the construction of an accurate pharmacophore model.[44] It is very much conserved across chemical series and is characterized by a basic sp_3 nitrogen (blue circle in Scheme 1 and Figure 1) acting as a main anchor, most probably through salt bridge formation with Asp3.32. At a distance of 4−5 Å, equivalent to four bonds in linear arrangement, an electron rich entity, typically an ether or a carbonyl function (red circle in Scheme 1 and Figure 1), is often observed. Optionally, a second basic nitrogen (e.g., **1**) can be present at a distance of 10−11 Å from the first one, most probably interacting with Glu5.46 (see Figure 1). As this glutamate residue is only present in H_3R and H_4R, this favorable interaction may also increase potency and selectivity over H_1R and H_2R. Alternatively, a second electron rich entity (e.g., **4**, **8**), probably interacting with Thr6.52, appears to be useful. Interestingly, this threonine residue is only present in H_3R. Between these two electron rich entities, several scaffolds such as naphthalene,[44] quinoline,[45] and indole were investigated and these demonstrated similar in vitro profiles. However, the naphthalene scaffold resulted in a rather large amphiphilic vector,[45,46] raising concerns about toxicological liabilities such as phospholipidosis. Moreover, our naphthalene series did not lead to efficacious compounds in a rodent model of obesity, after oral application.

Scheme 10. Preparation of 6-Hydroxy-2-carboxamideindole[a]

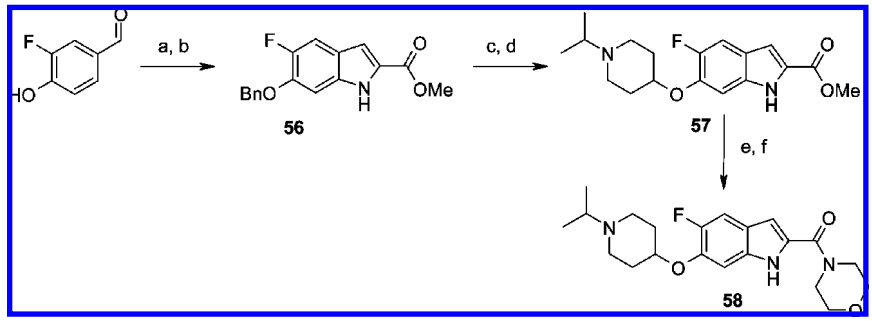

[a] (a) Benzyl bromide 1.1 equiv, potassium carbonate 1.2 equiv, DMF, 55 °C, 2 h, quant; (b) ethyl azidoacetate 4.6 equiv, NaOMe 4.1 equiv, toluol, methanol 0 °C, 3 h, then *p*-xylene, reflux, 2 h, 35%; (c) Pd/C 10% 0.03 equiv, ethyl acetate, H_2, room temp, 2 h, 74%; (d) 1-isopropyl-3-piperidinol 1.3 equiv, azodicarbonyldipiperidine 2.0 equiv, tri-*n*-butylphosphine 2.0 equiv, THF, room temp, 22 h, 48%; (e) $LiOH \cdot H_2O$ 1.1 equiv THF, water, reflux, 1 h, quant; (f) morpholine 1.2 equiv, TBTU 1.2 equiv, *i*-Pr_2NEt 6.0 equiv, room temp, 17 h, 68%.

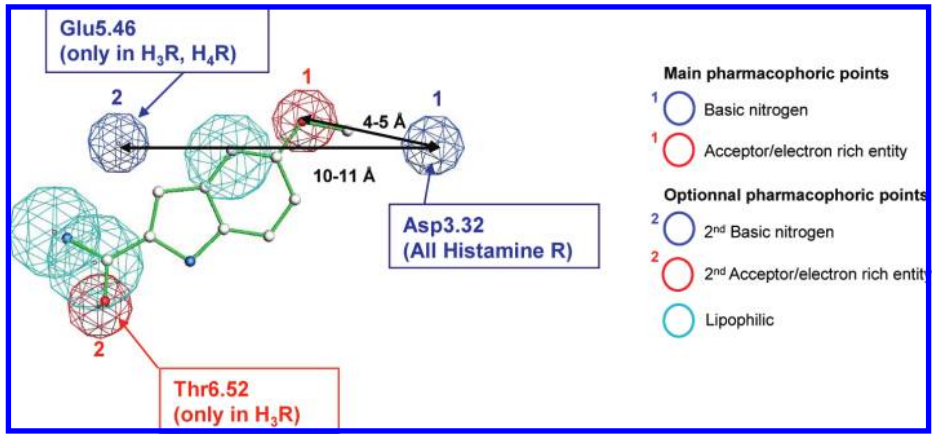

Figure 1. Description of a unique pharmacophore model. Various cores were docked to this pharmacophore semiautomatically and selected based on fitting and chemical tractability. On the basis of this, the 5-oxy-indole-2-carboxylic acid amide series was selected.

On the other hand, some of our H_3R ligands based on the quinoline core were associated with in vitro phototoxicity (data not shown). Both amphiphilic vector and in vitro phototoxicity are only surrogate markers of potential toxicity. However, the perspective to *fail late*, i.e., in toxicological studies, motivated us to identify alternatives. Characterized by lower lipophilicity compared to naphthalenes (clogP = 2.13 vs 3.32 for the core) and a distinct electronic density compared to quinolines, the indole central core additionally held the promise of an easy access to a third attachment point on the indole nitrogen, so far poorly explored, and an excellent chemical tractability.

First Attempts. Popularized by others, since it excellently fits the pharmacophore requirements with respect to the distance between the basic nitrogen and a first electron rich entity,[16c] the *N*-propoxypiperidine was first introduced together with a morpholine amide at the 2-position. To our delight, **20** was found to be an inverse agonist (hH_3R EC_{50} = 54 nM) with a high degree of selectivity toward the related H_1R, H_2R, and H_4R isoforms (6%, 3%, and 4% inhibition at 3 μM, respectively), securing the 5-oxyindole-2-carboxylic acid amide as a selective scaffold. Expecting a gain in entropy by restricting free rotation,[29a] the linear *n*-propyl chain was replaced by a more rigid piperidine. Indeed, more than 1 log-unit affinity improvement was measured for **25**, both in rat and in human receptor (hH_3R K_i = 5 nM and hH_3R K_i = 7 nM; see Table 1). Actually, species discrepancies minimally affected binding affinities for all the compounds described herein (below 10-fold difference; see Table 1).

Additionally, subnanomolar functional activity for **25** and good to excellent metabolic stability in rat and human microsomes preparation (12 and <1 (μL/min)/mg protein, respectively) warranted evaluation of its in vivo efficacy.

An acute model of obesity did not seem appropriate to characterize H_3R antagonists/inverse agonists. Therefore, we turned our attention toward the widely used dipsogenia assay. Thus, first-line in vivo screening was based on the antagonist/inverse agonist reversion of the water-intake induced by the H_3R selective agonist (*R*)-α-methylhistamine RAMH in rat (for assay setup, see Figure 2).[47] To our delight, **25** was also able to block the RAMH-induce water intake (inhibition was 91% at 30 mg/kg ip; see Figure 2).

Further profiling included inhibition of the human ether-a-go-go-related gene (hERG) channel, a marker for potential cardiac arrhythmia, which was a show-stopper in some competitor projects (vide supra). **25** showed only a modest inhibition of the hERG channel (28% at 10 μM).

However, oral application of **25** at a dose of 30 mg/kg b.i.d. for 3 days in a DIO rat did not induce any significant reduction in food intake or body weight. Although the compound was able to permeate the CNS (brain to plasma ratio of 0.3; brain exposure at 2 h postdosing at 30 mg/kg ip, 2228 ng/g), pharmacokinetic analysis revealed a fast metabolism (Cl_{int} = 50 (mL/min)/kg) and a short half-life ($t_{1/2}$ = 1 h). We hypothesized that a longer half-life was required to cover the whole active period of the animal (i.e., 12 h during the dark phase) and started seeking compounds with such characteristics. It is worth mentioning that the dipsogenia assay, lasting only 2 h, does not have the same requirement for a prolonged half-

Table 1. Structure−Activity Relationship of Selected Compounds[d]

compd	pK_a	log *D* at pH 7.4	hH_3R K_i (nM)[a]	rH_3R K_i (nM)[a]	hH_3R EC_{50} (nM)[a]	Cl micros Human ((μL/min)/mg)	Cl micros Rat ((μL/min)/mg)	dipso inhib (% at mg/kg ip)
20	10.0	0.32	71	91	54	<1	6	66 at 10
21	7.7	1.95	2	2	4	5	347	nt
22	10.0	0.03	4	4	6	10	13	nt
25	10.0	0.09	5	7	<1	<1	12	91 at 30
26	9.7	1.75	6	53	<1	10	55	76 at 10
27	9.9	0.59	9	37	9	5	20	70 at 30
28	9.8	−0.15	8	14	1	12	5	83 at 30
29	10.0	1.23	2	3	3	<1	17	86 at 10
30	9.7	1.2	2	3	4	5	9	58 at 1
31	nt	nt	7	7	6	nt	nt	nt
32	9.7	0.31	33	95	23	1	8	60 at 10
33	9.7	1.1	3	1	4	<1	13	87 at 10[c]
35	9.7	2.08	3	1	4	2	8	49 at 3
36	9.9	1.67	7	5	5	4	12	80 at 3
37	nt	nt	13	5	7	<1	nt	nt
38	9.6	1.31	3	4	4	<1	10	81 at 3[c]
39	nt	3.04	2	4	11	<1	20	nt
40	9.8	1.13	3	2	2	<1	16	nt
41	nt	3.38	1	0.3	2	<1	104	nt
42	9.6	0.35	11	5	4	1	4	nt
45	9.1	2.09	1	0.2	2	4	28	nt
46	6.4	1.83	23	13	9	8	228	nt
47	7.5	2.79	2	0.4	2	11	143	nt
49	9.9	−0.7	64	28	44	5	9	99 at 30
50	nt	nt	19[b]	nt	nt	nt	nt	nt
51	nt	0.04	2	7	5	<1	15	nt
53	6.8	1.97	7	5	3	10	16	93 at 10[c]
55	9.8	−0.12	86	nt	405	<1	15	nt
58	9.5	0.61	366	nt	112	6	18	nt

[a] K_i and EC_{50} were calculated from dose−response curves. [b] Percentage inhibition measured at 3 μM. [c] Per os application. Water intake increase in absence of RAMH stimulation. [d] nt: not tested.

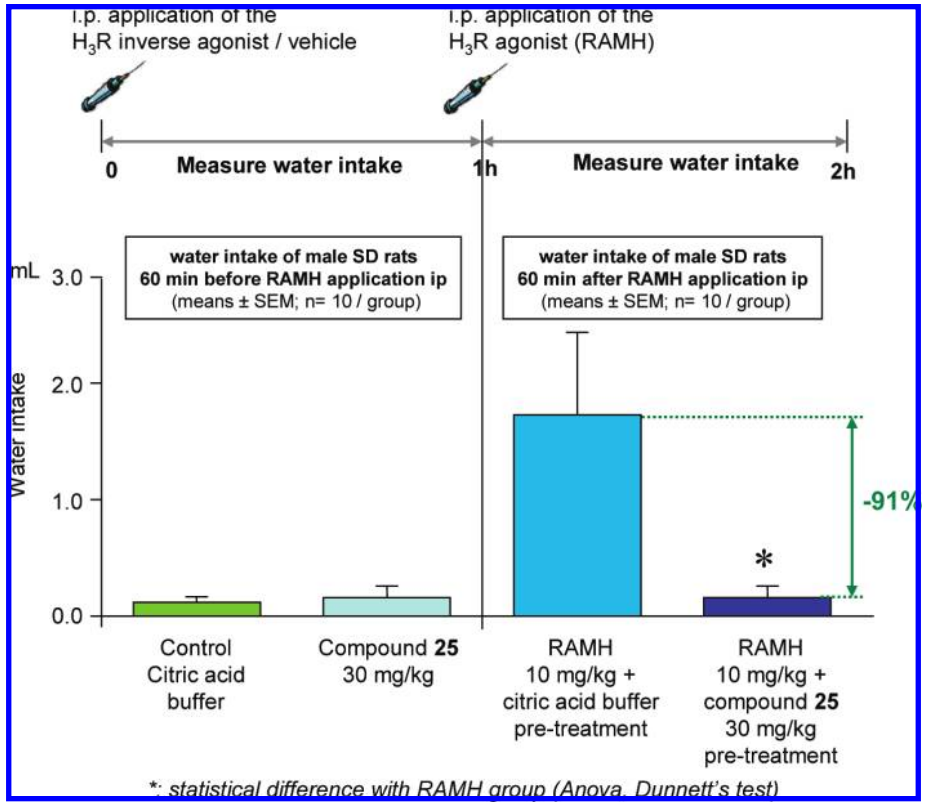

Figure 2. Dipsogenia as the acute pharmacological model. Principle is the reversal of H_3R-induced short-term water intake using an H_3R antagonist/inverse agonist. The H_3R inverse agonist is applied ip at $t = 0$, and water intake is recorded automatically (cf. Experimental Section) during 1 h (green bar) and compared with vehicle treated group (gray bar). The compound-treated groups do not exhibit significant modification of their water intake. Then RAMH, a H_3R selective agonist, is applied ip and water intake is again recorded for 1 h (light-blue bar). Percentage inhibition is calculated for the antagonist/inverse agonist-treated groups (dark-blue bars) relative to the group treated solely with RAMH (light-blue bar). A significant 91% inhibition is observed for compound **25** at a dose of 30 mg/kg ip.

life and that discrepancies between this first line assay and the longer 3-day food intake experiment were therefore not unexpected.

Replacement of the 5-oxy by the 5-amino group impacted the binding slightly negatively but did not prevent **49** from fully blocking the RAMH-induce water intake (inhibition of 99% at

30 mg/kg ip). However, **49** showed a high blood-to-plasma ratio (68-fold), presumably due to active accumulation in erythrocytes. Risk of blood toxicity excluded this compound from further development. Interestingly, this finding was highly compound specific; minor modifications (e.g., replacement of the morpholine ring by a pyrrolidine) prevented this accumulation (data not shown). On the other hand, N-alkylation of the 5-amino residue abolished any hH_3R binding affinity (see compound **50**, 19% inhibition at 3 μM on hH_3R, Table 1).

Exchange of the Attachment Point on the Indole Ring. With **25** as a reference compound, the effect of the attachment point on the indole was studied. Shifting the *N*-isopropyl-4-piperidineoxy from the 5- to the 6-position (indole numbering; see compound **32**, Table 1) weakened the binding on human receptor from 5 to 33 nM. Introduction of fluorine to block the reactive 5-indole position further decreased the affinity to H_3R and, counterintuitively, reduced the stability in human microsomes preparation as well ($Cl_{h.micros}$ = 1 (μL/min)/mg protein for **32** to 6 (μL/min)/mg protein for **58**; see Table 1).

Moving the carbonylmorpholine on the indole from the 2- to the 3-position did not affect the affinity but had a dramatic impact on the efficacy, although **55** was still classified as an inverse agonist (hH_3R EC_{50} = 405 nM). All these observations were in agreement with the pharmacophore model proposed above.

Investigations around the Amide. Lipophilic azepane **26** is extensively metabolized in vitro. Evaluation of the morpholine replacements, maintaining the local hydrophilicity (e.g., carbonyl-4-methoxypiperidine **27** or carbonylpyrrolidyl-3-ol **28**), did not help in improving the metabolic stability compared to **25**. Therefore, we attempted to *shield* the amide using polyfluorinated rings. Such an approach could lead to a dramatic reduction of the aqueous solubility, hampering further development. However, driven by the basic amine, solubility was in general not an issue within this series. Thus, carbonyl-4,4′-difluoropiperidine **30** was soluble (>540 mg/L in LYSA assay), potent on the H_3R receptor (hH_3R K_i = 2 nM), and metabolically stable in vitro ($Cl_{h.micros}$ = 5 (μL/min)/mg protein; $Cl_{r.micros}$ = 9 (μL/min)/mg protein; see Table 1). Its pharmacokinetic profile combined an acceptable intrinsic clearance (Cl_{int} = 18 (mL/min)/kg), a perfect bioavailability (~100%), and an extended half-life ($t_{1/2}$ = 4 h). More interestingly, this compound was active in our 3-day obesity model at 10 mg/kg b.i.d. after ip application (12% reduction in food intake), despite a reduced brain exposure compared to **25** (brain exposure 2 h postdosing at 10 mg/kg ip, 1615 ng/g), strengthening our working hypothesis concerning the importance of the half-life for efficacy (vide supra). Further, po application did not alter the efficacy or the exposure during the 3-day obesity model (10% reduction in food intake; brain exposure 2 h postdosing at 10 mg/kg po, 1692 ng/g), ruling out an obvious taste aversion effect on food intake. However, 73% inhibition of the hERG channel at 10 μM was considered as being suboptimal for this indication.

***N*-Indole Substituant as a Third Attachment Point.** Acylation of *N*-indole generated compounds that were slightly chemically unstable in basic aqueous media (compound **37**). However, sulfonylation (e.g., compound **38**) provided molecules with an excellent overall profile. Most importantly, the half-life of **38** reached 6 h and, to our delight, was found to be highly efficacious in our 3-day obesity model (14% reduction of food intake at 10 mg/kg po b.i.d.). However, hERG affinity was still of concern with 64% inhibition at 10 μM. The isopropyl derivative **36** exhibited an excellent in vitro profile as well. Intrinsic clearance of **38** and **36** was identical, but the larger volume of distribution (V_{ss} = 9.2 L·kg^{-1}) for the latter led to an extended half-life ($t_{1/2}$ = 11 h). A food intake reduction of 17% at 10 mg/kg po b.i.d. was recorded (brain exposure 2 h postdosing at 10 mg/kg po, 1274 ng/g). hERG affinity was improved to 42% inhibition at 10 μM. *N*-2,2,2-trifluoroethylindole **35** led to undesired side effects in the IRWIN-type safety assay and was discarded,[48] whereas replacement of the difluoropiperidine by a morpholine did not exhibit any side effects at the same dose (30 mg/kg ip). In line with a short half-life ($t_{1/2}$ = 1.8 h) and despite an inhibition of 87% at 10 mg/kg ip (brain exposure 2 h postdosing at 10 mg/kg ip, 435 ng/g) in the dispogenia assay, **33** was not active in the subchronic obesity model at 10 mg/kg po b.i.d. *N*-Indole substitution proved to be very tolerant with respect to both size and electronic properties. However, large N-substituents hampered the selectivity toward H_2R (cf. compounds **39** and **41**, >30% inhibition at 3 μM) and were therefore no longer pursued.

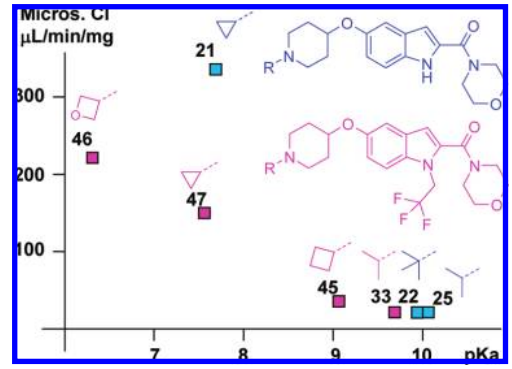

Figure 3. Rat microsomal clearance is negatively correlated with the measured pK_a (two subseries in blue and magenta).

Variations on the Basic Side Chain: Consequences on Microsomal Clearance and hERG Affinity. Replacement of the isopropyl group by cyclobutyl modestly reduced the pK_a (9.1 for **45** vs 9.7 for **33**), although the stronger electron withdrawing cyclopropyl dramatically reduced the pK_a (e.g., for **21**, pK_a = 7.7; for **47**, pK_a = 7.5). Similarly, the potent binder **46** (hH_3R K_i = 23 nM) was identified with a pK_a as low as 6.4, the lowest value within this series. In contrast, electron-donating *N*-*tert*-butyl increased the basicity significantly without large alteration of the affinity (compound **22**: pK_a = 10.0; hH_3R K_i = 4 nM). Thus, within a pK_a range spanning more than 3 log units, no correlation could be drawn between pK_a and hH_3R K_i, although it is assumed that within the receptor binding pocket these H_3R inverse agonists are protonated, forming a salt bridge with Asp 3.32.

Clearance for **46** and **47**, particularly in rat microsomal preparations, was poor (228 and 143 (μL/min)/mg protein, respectively). Although only loose correlation was observed between microsomal clearance and log *D*, it turned out that microsomal clearance was negatively and almost linearly correlated with the pK_a (two subseries in blue and magenta; see Figure 3). Introduction of local polarity (e.g., compound **46**) or increased s-bond character (e.g., compounds **21** and **47**) does not appear to improve metabolic stability. These data suggest that metabolic stability is exclusively dictated by the pK_a for this series.

Encouraged by this observation to introduce more drastic changes on the basic side chain, the 4-piperidineoxy moiety was replaced by a *N*-carbonylpiperazine. Although **53** was not optimal as far as microsomal stability was concerned, inhibition in the dipsogenia assay was excellent (93% at 10 mg/kg po). The in vivo intrinsic clearance was acceptable (Cl_{int} = 24 (mL/min)/kg), and **53** also penetrated the brain (brain/plasma of 0.3);

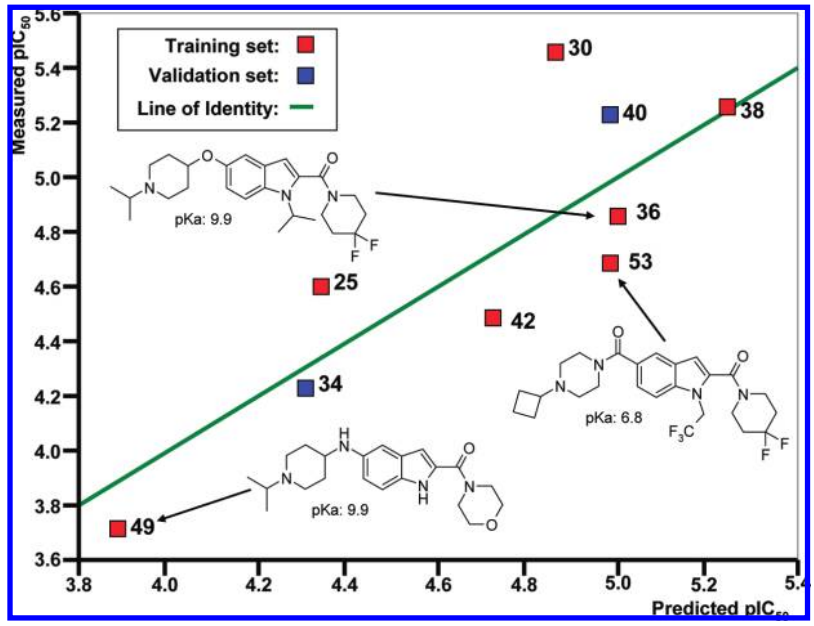

Figure 4. Correlation of experiment vs calculated hERG pIC_{50}, using Roche automatic SAR analyzer (ROSARA). The model is relying solely on two descriptors, the percentage of membrane-bound compound in the parallel artificial membrane assay (PAMPA), and log *D* and is independent of pK_a. Red squares represent compounds used to develop the model (training set). Blue squares represent compounds used to validate it (validation set). The line of identity is represented in green, with a regression coefficient of 0.736 (based on the training set).

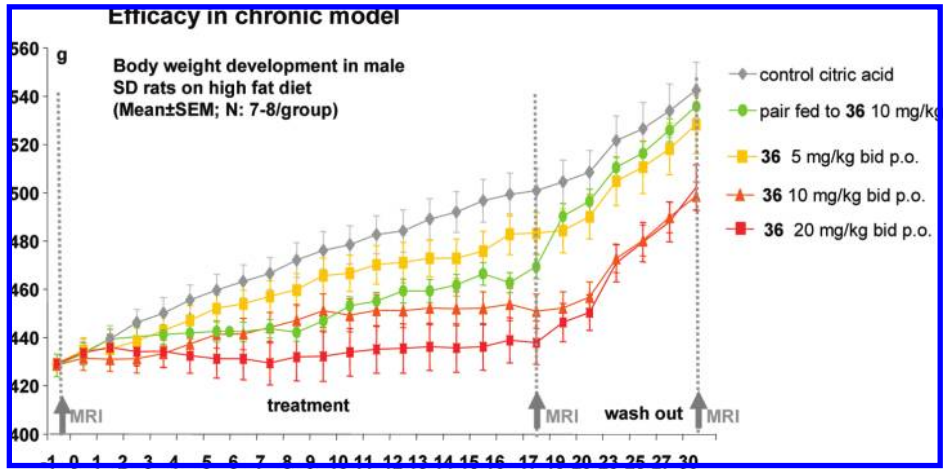

Figure 5. Chronic dosing with compound **36** at 5, 10, and 20 mg/kg b.i.d. po in a diet-induced obesity rat model. Dose dependent reduction in body weight was observed. The body weight development for the 10 mg/kg group and the pair-fed group was comparable. The rebound effect observed after stopping treatment was less marked with the treated groups than with the pair-fed group.

however, the low protein binding (52% in rat) and the low V_{ss} (1.5 L/kg) shortened the half-life. Therefore, inefficacy of **53** in the subchronic food intake model at 10 mg/kg po b.i.d. was somewhat expected. hERG inhibition of **53** was reduced (33% at 10 μM).

Such a data set suggested keeping a rather basic nitrogen (i.e., $pK_a \approx 9-10$) and replacing the morpholine by difluoropiperidine for optimal metabolic stability in vitro. Concerning hERG, a basic nitrogen is often considered as the *usual culprit*, although definitely not the only one.[49] To gain a better understanding of the main driver for hERG inhibition, we applied the Roche automatic SAR analyzer (ROSARA).[50] This proprietary software, based on the use of partial least squares analysis, is designed to study potential correlation between a defined compound property (i.e., hERG inhibition in this case) and numerous descriptors. These descriptors can be both measured (e.g., LYSA solubility, log *D*, hH_3R K_i, pK_a, etc.) or calculated (e.g., clogP, PSA, etc.). In our case, ROSARA was able to generate a valuable hERG model by selecting only two in vitro descriptors: the percentage of membrane-bound compound in the parallel artificial membrane assay (PAMPA)[51] and log *D*. As some small molecule hERG inhibitors are assumed to interact with the hERG channel through the membrane section, this result made a lot of sense. Translation of hERG single point values measured at 10 μM into pIC_{50} values significantly improved the regression coefficient to 0.736. Interestingly, although the pK_a in the training set spanned more than 3 log units, no correlation with hERG affinity was observed. The model has been validated with two new compounds from the same series (compounds **34** and **40**, blue squares; see Figure 4) and then routinely applied not to select but to prioritize candidates at an early stage (before in vivo experiments). The independence of pK_a and hERG inhibition, together with the improved metabolic stability for compounds having $pK_a > 9$ (vide supra), biased us toward the selection of rather basic ligands.

Characterization of Compound 36. Among those compounds, **36** attracted our attention for its striking combination

of potent H_3R binding (hH_3R K_i = 7 nM; rH_3R K_i = 5 nM), low clearance in vivo (intrinsic clearance in rat, 10 (μL/min)/mg protein), extended half-life ($t_{1/2}$ = 11 h in rat), rather low hERG inhibition (42% hERG inhibition at 10 μM), and ultimately excellent performance in the 3-day obesity model (17% reduction in food intake at 10 mg/kg po b.i.d.).

To evaluate whether food intake is decreased in a specific manner or by disruption of normal feeding behavior in a nonspecific manner (e.g., by inducing sedation, hyperactivity, or any other motor effects that could interfere with food intake), the effect of **36** was recorded on the different components of the behavioral satiety sequence (BSS).[52] Compound **36** was tested at three different doses (10, 20, 30 mg/kg po) and compared to the vehicle treated group. At all tested doses, administration of **36** did not cause a disruption of the behavioral pattern of rats, providing confidence that reduction of food intake was achieved by enhancing natural satiety in a specific manner.

To test **36** in a disease relevant model, male Sprague−Dawley rats were fed with a high fat diet (HFD, 43% of energy as fat, 19% w/w fat) 10 weeks prior to the treatment period and during dosing. Chronic application of **36** (5, 10, and 20 mg/kg b.i.d. po) for 17 days in this diet induced obesity rat model (DIO) led to a dose-dependent slower progression of body weight in all groups (−4%, −10%, −13%, respectively), statistically significant for the 10 and 20 mg/kg groups (cf. Figure 5). A pair-fed group (a group of animals receiving exactly the amount of food eaten by the 10 mg/kg group) was incorporated into the study. As expected, the body weight gains for the 10 mg/kg group (orange line) and the pair-fed group (green line) were comparable. The body weight was still recorded for 13 days after withdrawal of the treatment. Interestingly, the rebound effect observed after stopping treatment was less marked with the treated groups than with the pair-fed group.

Conclusion

A series of 5-hydroxyindole-2-carboxylic acid amide derivatives was identified as a novel class of H_3R inverse agonist.[53] By reliance on a pharmacophore model built on public information, the indole scaffold, in addition to other scaffolds,[43−45] was identified as a promising chemical entry point. Following SAR development, extensive multidimensional optimization, and careful evaluation of the underlying drivers of microsomal clearance and hERG affinity, **36** proved to combine the best overall characteristics for further profiling. In an indirect acute pharmacodynamic model, **36** reversed dose-dependently the water intake induced by an H_3R selective agonist (RAMH). Furthermore, in a 17-day diet-induce obesity (DIO) rat model, **36** demonstrated a robust reduction in body weight gain after po application and showed a reduced rebound effect compared to a per-fed group. On the basis of its efficacy, metabolic stability, and safety profile, compound **36** was selected for further in depth evaluation.

Experimental Section

Chemistry. General. Proton NMR spectra were obtained on Bruker 300 or 400 MHz instrument with chemical shifts (δ in ppm) reported relative to tetramethylsilane as an internal standard. NMR abbreviations are as follows: s, singlet; d, doublet; t, triplet; quad, quadruplet; quint, quintuplet; sext, sextuplet; hept, heptuplet; mult, multiplet.

Elemental analyses were performed by Solvias AG (Mattenstrasse, Postfach, CH-4002 Basel, Switzerland). Column chromatography was carried out on silica gel 60 (32−60 mesh, 60 Å) or on prepacked columns (Isolute Flash Si). Mass spectra were recorded on SSQ 7000 (Finnigan-MAT) for electron impact ionization.

Detailed Description. 5-(1-Isopropylpiperidin-4-yloxy)-1*H*-indole-2-carboxylic Acid Ethyl Ester (23). To a cold (ice−water) solution of 5-hydroxyindole-2-carboxylic acid ethyl ester (20 g, 97 mmol) and triphenylphosphine (30.68 g, 117 mmol, 1.2 equiv) in tetrahydrofuran (500 mL) was added dropwise a solution of di-*tert*-butyl azodicarboxylate (26.93 g, 117 mmol, 1.2 equiv) in tetrahydrofuran (100 mL). The mixture was stirred for 2 days at room temperature and concentrated in vacuo. Purification was performed by column chromatography on silica gel using a gradient of dichloromethane/methanol/aqueous ammonia (19:1:0 to 95:5:0.25) as eluant to afford, after evaporation, a colorless oil (40.26 g). This oil was dissolved in ethyl acetate and concentrated in vacuo to ∼50 mL. Methyl *tert*-butyl ether was added, and the mixture was stirred at ∼0−3 °C (ice bath) and then filtered and dried in vacuo to afford the desired product as a white solid (21.53 g, 67%). ^{1}H NMR (400 MHz, $CDCl_3$) δ 8.77 (s broad, 1H); 7.30 (d, J = 8 Hz, 1H); 7.15−7.10 (mult, 2H); 7.00 (dd, J = 8 Hz, 2 Hz, 1H); 4.40 (quad, J = 7 Hz, 2H); 4.26 (hept, J = 4 Hz, 1H); 2.87−2.76 (mult, 2H); 2.75 (hept, J = 8 Hz, 1H); 2.42−2.33 (mult, 2H); 2.08−1.98 (mult, 2H); 1.87−1.77 (mult, 2H); 1.41 (t, J = 7 Hz, 3H); 1.06 (d, J = 6 Hz, 6H) ppm. MS (EI) *m/e*: 331.1 $(M + H)^+$.

5-(1-Isopropylpiperidin-4-yloxy)-1*H*-indole-2-carboxylic Acid, Hydrochloride Salt, with Lithium Chloride. To a solution of 5-(1-isopropylpiperidin-4-yloxy)-1*H*-indole-2-carboxylic acid ethyl ester (**23**, 10.0 g, 30 mmol) in a mixture of tetrahydrofuran (130 mL) and methanol (27 mL) was added a solution of lithium hydroxide monohydrate (1.40 g, 33 mmol, 1.1 equiv) in water (65 mL). The mixture was stirred for 1 h at reflux and concentrated in vacuo. The pH of the resulting suspension was adjusted to pH 2 with hydrochloric acid (2 N). The solution was dried in vacuo to afford the desired product as a brown solid (11.6 g, quant.). This solid was used in the next step without further purification. ^{1}H NMR (300 MHz, DMSO-d_6) δ 11.67 (s, 1H); 7.35 (d, J = 9 Hz, 1H); 7.23 (broad s, 1H); 6.97 (d, J = 1 Hz, 1H); 7.00−6.90 (mult, 1H); 4.85−4.75 (mult, 1H); 3.46 (hept, J = 7 Hz, 1H); 3.25−3.15 (mult, 4H); 2.30−2.20 (mult, 2H); 2.10−2.00 (mult, 2H); 1.31 (d, J = 7 Hz, 6H) ppm. MS (EI) *m/e:* 301.2 $(M\text{-}H)^-$.

(4,4-Difluoropiperidin-1-yl)[5-(1-isopropyl-piperidin-4-yloxy)-1*H*-indol-2-yl]methanone (30). To a solution of 5-(1-isopropylpiperidin-4-yloxy)-1*H*-indole-2-carboxylic acid, hydrochloride salt, with lithium chloride (5.0 g, 13 mmol) and 2-(1*H*-benzotriazole-1-yl)-1,1,3,3-tetramethyluronium tetrafluoroborate (5.3 g, 15.7 mmol, 1.2 equiv) in *N*,*N*-dimethylformamide (75 mL) were added ethyldiisopropylamine (11.5 mL, 65.6 mmol, 5.0 equiv) and 4,4′-difluoropiperidine hydrochloride (2.48 g, 15.7 mmol, 1.2 equiv). The mixture was stirred overnight at room temperature and partitioned between saturated aqueous sodium hydrogenocarbonate solution (300 mL) and ethyl acetate (300 mL). The aqueous layer was extracted with ethyl acetate, and the combined organic phases were washed with water and brine, dried over sodium sulfate, filtered, and concentrated to ∼40 mL. Methyl *tert*-butyl ether (40 mL) was added with stirring, and the precipitate was filtered, washed with cold (5−10 °C) methyl *tert*-butyl ether, and dried in vacuo to afford the desired product as a white solid (4.95 g, 93%). ^{1}H NMR (300 MHz, $CDCl_3$) δ 8.97 (s, 1H); 7.32 (d, J = 9 Hz, 1H); 7.11 (d, J = 2 Hz, 1H); 6.99 (dd, J = 9 Hz, 2 Hz, 1H); 6.69 (d, J = 2 Hz, 1H); 4.24 (hept, J = 4 Hz, 1H); 4.08−3.95 (mult, 4H); 3.87−3.70 (mult, 3H); 2.42−2.35 (mult, 2H); 2.19−1.97 (mult, 6H); 1.92−1.75 (mult, 2H); 1.06 (d, J = 7 Hz, 6H) ppm. MS (EI) *m/e:* 406.2 $(M + H)^+$. Anal. ($C_{22}H_{29}N_3O_2$) C, H, N.

(4,4-Difluoropiperidin-1-yl)[1-isopropyl-5-(1-isopropylpiperidin-4-yloxy)-1*H*-indol-2-yl]methanone (36). To a solution of (4,4-difluoropiperidin-1-yl)[5-(1-isopropylpiperidin-4-yloxy)-1*H*-indol-2-yl]methanone (**30**, 1.5 g, 3.7 mmol) in *N*,*N*-dimethylformamide (18 mL) was added sodium hydride (50% w/w dispersion in oil, 178 mg, 4.1 mmol, 1.1 equiv). The mixture was stirred 50 min at 70 °C before the addition of 2-bromopropane (0.55 mL, 4.4 mmol, 1.2 equiv). The mixture was stirred 18 h at 70 °C and partitioned between ethyl acetate and water. The aqueous layer was extracted with ethyl acetate, and the combined organic phases were washed with water, dried over sodium sulfate, filtered, and concentrated in

vacuo. Purification was performed by column chromatography on silica gel using a gradient of dichloromethane/methanol (1:0 then 19:1) as eluant to afford, after evaporation, the desired product as a white solid (984 mg, 59%). ^{1}H NMR (400 MHz, $CDCl_3$) δ 7.41 (d, J = 9 Hz, 1H); 7.09 (dd, J = 2 Hz, 1H); 6.92 (dd, J = 9 Hz, 2 Hz, 1H); 6.40(s, 1H); 4.73 (hept J = 7 Hz, 1H); 4.30−4.20 (mult, 1H); 3.87−3.78 (mult, 4H); 2.85−2.75 (mult, 2H); 2.74 (hept, J = 7 Hz, 1H); 2.38 (broad t, J = 9 Hz, 2H); 2.08−1.95 (mult, 6H); 1.87−1.75 (mult, 2H); 1.62 (d, J = 7 Hz, 6H); 1.05 (d, J = 7 Hz, 6H) ppm. MS (EI) *m/e:* 448.2 $(M + H)^+$. Anal. ($C_{25}H_{35}F_2N_3O_2$) C, H, N.

In Vitro Assays. H_1R, H_2R, H_3R, and H_4R Radioligand Binding Assays. For the rat H_3R and human H_1R, H_3R, and H_4R binding assays, membranes were prepared from recombinant CHO cells stably expressing the respective histamine receptor. Membranes for the H_2R binding assay were purchased at Euroscreen, Belgium. For H_3 receptor competition binding (human and rat), membrane preparations were incubated with [^{3}H]-(*R*)-α-methylhistamine (1.0 nM for human H_3R, 2.0 nM for rat H_3R) in the presence or absence of increasing concentrations (10 concentrations over a 4.5 log-unit range) of ligands for 120 min at 25 °C in a final volume of 0.2 mL of 50 mM Tris-HCl, 5 mM $MgCl_2$, pH 7.4, buffer, gently shaking. Nonspecific binding was defined with 5 μM (*R*)-(−)-α-methylhistamine. Cloned human histamine H_1 receptor radioligand binding assays were performed using 1.5 nM [^{3}H]pyrilamine for 30 min in 50 mM Tris-HCl, 2 mM $MgCl_2$, 20 mM NaCl, and 250 mM sucrose, pH 7.4. Nonspecific binding was defined with 10 μM pyrilamine. Cloned human H_2 receptor binding assays were performed using 13 nM [^{3}H]tiotidine for 60 min in 50 mM Tris-HCl, 500 mM NaCl, pH 7.4. Nonspecific binding was defined with 100 μM tiotidine. Cloned H_4 receptor binding was performed using 25 nM [^{3}H]histamine for 60 min in 50 mM Tris-HCl, 5 mM EDTA, 250 mM sucrose, pH 7.4. Nonspecific binding was defined with 100 μM histamine. All binding reactions were terminated by vacuum filtration onto polyethylenimine (0.3% and 0.5% for H_4 receptor binding only) presoaked GF/B filter plates (Packard) followed by three brief washes with 2 mL of ice-cold binding buffer with the exception that the binding buffer for the H_1 and H_3 receptors contained 500 mM NaCl. Liquid scintillation counting was used to determine bound radiolabel. IC_{50} values and Hill slopes were determined by a four parameter logistic model using ActivityBase (ID Business Solution, Ltd.). pK_i values were determined by the generalized Cheng−Prusoff equation (Cheng and Prusoff, 1973).

H_3R GTPγS-Binding Assay. This assay was performed to determine the activity of compounds at human H_3 receptors using membranes from CHO cells (Euroscreen, Belgium). After thawing, the membranes were suspended in 20 mM HEPES−NaOH buffer (pH7.4) containing 1 mM $MgCl_2$, 100 mM NaCl, 45 μg/mL saponin and 10 μM GDP. Membrane suspension and wheat germ agglutinin SPA beads (Amersham) were mixed (beads, 13 mg/mL; membranes, 150 μg protein/mL). GTPγ^{35}S binding was performed in 96-well microplates in a total volume of 180 μL with 30 μg of membrane proteins and 0.28 nM GTPγ^{35}S. Nonspecific binding was measured in the presence of 10 μM cold GTPγS. Plates were sealed and agitated (350 rpm) at room temperature for 2 h. The beads were then settled by centrifugation (1000 rpm, 10 min), and the plate was counted in a Top count using quench correction.

Rat and Human Microsomal Clearances. Human or rat microsome incubations were conducted by an automated procedure implemented on a Genesis workstation (Tecan, Switzerland). Compounds (2 μM) were incubated in microsomes at 0.5 mg protein/mL in a 50 mM potassium phosphate buffer, pH 7.4, at 37 °C. Cofactor (NADPH) was produced by a generating system (glucose 6-phosphate, 3.2 mM; β-NADP, 2.6 mM; $MgCl_2$, 6.5 mM). Addition of the NADPH generating system to the prewarmed microsomes containing the test compound started the reaction. Aliquots (50 μL) were taken at six defined time points within 30 min and transferred into 100 μL of methanol containing an internal standard. Concentration of each compound was analyzed by LC−MS/MS using a Synergy-4-Polar RP 18 column (Phenomenex, Torrance, CA). Quantitative detection was achieved on a SCIEX 2000 instrument (MDS Sciex, Concord, ON, Canada) using electron spray ionization. Concentrations were determined by ratio of test compound and internal standard peaks and given as a percentage of the concentration measured at the first time point (substrate depletion). Intrinsic clearance (CL_{int}, in (μL/min)/mg microsomal protein) is the rate constant of the first-order decay of the test compound, normalized for the protein concentration in the incubation.

In Vivo Assays. Animals. Male Wistar rats around 350 g body weight (11 and 13 weeks of age) were used for the dispogenia studies. For the food intake studies male Sprague−Dawley (SD) rats were put on a high fat diet (HFD, KLIBA 2157, 43% of energy as fat, 19% w/w fat) for 2 weeks until use. For the chronic experiments 100 male DIO SD rats were used. All animals were obtained from Iffa Credo/Charles River, France. Animals were put on HFD (KLIBA 2157, 43% of energy as fat, 19% w/w fat) at 3 weeks of age for 10 weeks and on a reversed light cycle (9.30 a.m. lights off; 9.30 p.m. lights on). During the growing period, body weight was measured at the beginning of the high fat feeding and before the stratification. Responders to HFD were separated from nonresponder animals using the following criteria: the difference between average body weight of high responders and the body weight of rats fed standard chow diet was at least 2 times the standard deviation of the average body weight of the standard chow diet group.

Dipsogenia Assay. Rats (n = 10 animals/group) were tested for the inhibition of the (*R*)-α-methylhistamine (RAMH) induced short-term water intake in a dipsogenia model. Each rat was injected po or ip with either vehicle (citric acid buffer pH 3.3) or H_3R inverse agonists, and water intake was monitored automatically (TSE system) for 1 h. Afterward 10 mg/kg RAMH or 0.9% NaCl was administered ip and water intake was again monitored for 1 h.

Three-Day Food Intake. A subchronic, 3-day model for food intake in male SD rat on HFD was used to assess efficacy of H_3R inverse agonists. Animals were put on a reversed light cycle (9.30 a.m. lights off; 9.30 p.m. lights on) for 2 weeks, for adaptation. Access to tap water and food was ad libitum. Food intake and body weight were monitored daily 1 week prior to compound testing, and animals were stratified into homogeneous groups according to food intake and body weight. The compound was applied b.i.d. po at different doses 1 h prior light cycle change and 6 h later, and food intake was monitored daily for 3 consecutive days.

Chronic DIO SD Rat Model. To evaluate the long-term efficacy of H_3R inverse agonists on body weight development, food intake, body fat, and plasma parameters, a chronic DIO SD rat model was used. After separation of responders from nonresponders to the HFD, responders were adapted to their housing for 2 weeks for adaptation. In parallel, animals were monitored for food intake and body weight daily. Animals were stratified into homogeneous treatment groups according to their food intake, body weight, and body fat. In order to assess possible effects on body weight and fat depots beyond a reduction of food intake, a pair-fed group was run in parallel to the 10 mg/kg dose group, given the exact amount of food of the treatment group with a 24 h delay. Any improvement of the metabolic status would therefore be distinguishable from the effect of body weight reduction.

Acknowledgment. The authors thank Dr. Holger Fischer for his help during the use of Roche structure−activity relationship analyzer (ROSARA) and Dr. Liudmila Polonchuk for the measurement of the hERG channel inhibitions.

Supporting Information Available: Preparation details of all compounds described in Table 1 and their intermediates, together with spectroscopic data; table of elemental analysis data of target compounds; description of the pK_a measurement, lipophilicity determination (log D), lyophilization solubility assay (LYSA), hERG inhibition assay, rat pharmacokinetic measurement, and behavioral satiety sequence (BSS) method. This material is available free of charge via the Internet at http://pubs.acs.org.

References

(1) Carek, P. J.; Dickerson, L. M. Current concepts in the pharmacological management of obesity. *Drugs* **1999**, *57*, 883–904.

(2) (a) Spanswick, D.; Lee, K. Emerging antiobesity drugs. *Expert Opin. Emerging Drugs* **2003**, *8*, 217–237. (b) Kordik, C. P.; Reitz, A. B. Pharmacological treatment of obesity: therapeutic strategies. *J. Med. Chem.* **1999**, *42*, 181–201. (c) Das, S. K.; Chakrabarti, R. Antiobesity therapy: emerging drugs and targets. *Curr. Med. Chem.* **2006**, *13*, 1429–1460. (d) Halford, J. C. G. Obesity drugs in clinical development. *Curr. Opin. Invest. Drugs* **2006**, *7*, 312–318.

(3) (a) Centers for Disease Control and Prevention; U.S. Department of Health and Human Services. http://www.cdc.gov/. (b) Stein, C. J.; Colditz, G. A. The epidemic of obesity. *J. Clin. Endocrinol. Metab.* **2004**, *89*, 2522–2525.

(4) Mokdad, A. H.; Ford, E. S.; Bowman, B. A.; Dietz, W. H.; Vinicor, F.; Bales, V. S.; Marks, J. S. Prevalence of obesity, diabetes, and obesity-related health risk factors. *JAMA, J. Am. Med. Assoc.* **2003**, *289*, 76–79.

(5) Mokdad, A. H.; Marks, J. S.; Stroup, D. F.; Gerberding, J. L. Actual causes of death in the United States. *JAMA, J. Am. Med. Assoc.* **2004**, *291*, 1238–1245.

(6) Farrigan, C.; Pang, K. Obesity market overview. *Nat. Rev. Drug Discovery* **2002**, *1*, 257–258.

(7) Padwal, R. S.; Majumdar, S. R. Drug treatments for obesity: orlistat, sibutramine, and rimonabant. *Lancet* **2007**, *369*, 71–77.

(8) (a) Parsons, M. E.; Ganellin, C. R. Histamine and its receptors. *Br. J. Pharmacol.* **2006**, *147*, S127–S135. (b) Hill, S. J.; Ganellin, C. R.; Timmerman, H.; Schwartz, J. C.; Shankley, N. P.; Young, J. M.; Schunack, W.; Levi, R.; Haas, H. L. International Union of Pharmacology. XIII. Classification of histamine receptors. *Pharmacol. Rev.* **1997**, *49*, 253–278.

(9) For examples, see the following: (a) Bernstein, D. I.; Schoenwetter, W. F.; Nathan, R. A.; Storms, W.; Ahlbrandt, R.; Mason, J. Efficacy and safety of fexofenadine hydrochloride for treatment of seasonal allergic rhinitis. *Ann. Allergy, Asthma, Immunol.* **1997**, *79*, 443–448. (b) Harada, M.; Terai, M.; Maeno, H. Effect of a new potent H2-receptor antagonist 3[[[2-[(diaminomethylene)amino]-4-thiazolyl]methyl]thio]-N2-sulfamoylpropionamidine (YM-11170) on gastric mucosal histamine-sensitive adenylate cyclase from guinea pig. *Biol. Pharmacol.* **1983**, *32*, 1635–1640.

(10) Hough, L. B. Genomics meets histamine receptors: new subtypes, new receptors. *Mol. Pharmacol.* **2001**, *59*, 415–419.

(11) Liu, C.; Ma, X.-J.; Jiang, X.; Wilson, S. J.; Hofstra, C. L.; Blevitt, J.; Pyati, J.; Li, X.; Chai, W.; Carruthers, N.; Lovenberg, T. W. Cloning and pharmacological characterization of a fourth histamine receptor (H4) expressed in bone marrow. *Mol. Pharmacol.* **2001**, *59*, 420–426.

(12) (a) de Esch, I. J. P.; Thurmond, R. L.; Jongejan, A.; Leurs, R. The histamine H4 receptor as a new therapeutic target for inflammation. *Trends Pharmacol. Sci.* **2005**, *26*, 462–469. (b) Smits, R. A.; Lim, H. D.; Stegink, B.; Bakker, R. A.; de Esch, I. J. P.; Leurs, R. Characterization of the histamine H4 receptor binding site. Part 1. Synthesis and Pharmacological evaluation of dibenzodiazepine derivatives. *J. Med. Chem.* **2006**, *49*, 4512–4516. (c) Lim, H. D.; Smits, R. A.; Bakker, R. A.; van Dam, C. M. E.; de Esch, I. J. P.; Leurs, R. Discovery of *S*-(2-guanidylethyl)-isothiourea (VUF 8430) as a potent nonimidazole histamine H4 receptor agonist. *J. Med. Chem.* **2006**, *49*, 6650–6651. (d) Jablonowski, J. A.; Grice, C. A.; Chai, W.; Dvorak, C. A.; Venable, J. D.; Kwok, A. K.; Ly, K. S.; Wei, J.; Baker, S. M.; Desai, P. J.; Jiang, W.; Wilson, S. J.; Thurmond, R. L.; Karlsson, L.; Edwards, J. P.; Lovenberg, T. W.; Carruthers, N. I. The first potent and selective non-imidazole human histamine H4 receptor antagonists. *J. Med. Chem.* **2003**, *46*, 3957–3960.

(13) Arrang, J.-M.; Garbarg, M.; Schwartz, J.-C. Auto-inhibition of brain histamine release mediated by a novel class (H3) of histamine receptor. *Nature* **1983**, *302*, 832–837.

(14) Lovenberg, T. W.; Roland, B. L.; Wilson, S. J.; Jiang, X.; Pyati, J.; Huvar, A.; Jackson, M. R.; Erlander, M. G. Cloning and functional expression of the human histamine H_3 receptor. *Mol. Pharmacol.* **1999**, *55*, 1101–1107.

(15) (a) Mercer, L. P.; Kelley, D. S.; Humphries, L. L.; Dunn, J. D. Manipulation of central nervous system histamine or histaminergic receptors (H1) affects food intake in rats. *J. Nutr.* **1994**, *7*, 1029–1036. (b) Lecklin, A.; Etu-Seppala, P.; Stark, H.; Tuomisto, L. Effects of intracerebroventricularly infused histamine and selective H1, H2, and H3 receptor agonists on food and water intake and urine flow in Wistar rats. *Brain Res.* **1998**, *279*, 288.

(16) For reviews, see the following: (a) Leurs, R.; Blandina, P.; Tedford, C.; Timmerman, H. Therapeutic potential of histamine H3-receptor agonists and antagonists. *Trends Pharmacol. Sci.* **1998**, *19*, 177–183. (b) Leurs, R.; Timmerman, H. The Histamine H3-Receptor: A Target for New Drugs. In *Pharmacochemistry Library*; Elsevier: Amsterdam, 1998; Vol. 30. (c) Stark, H.; Arrang, J. M.; Ligneau, X.; Garbarg, M.; Ganellin, C. R.; Schwartz, J. C.; Schunack, W. The Histamine H3-Receptor and Its Ligands. In *Progress in Medicinal Chemistry*; King, F. D., Oxford, A. W., Eds.; Elsevier: Amsterdam, 2001; Vol. 38, pp 279−309. (d) Esbenshade, T. A.; Fox, G. B.; Cowart, M. D. Histamine H_3 Receptor Antagonists: Preclinical Promise for Treating Obesity and Cognitive Disorders. *Mol. Interventions* **2006**, *6*, 77–88. (e) Esbenshade, T. A.; Browman, K. E.; Bitner, R. S.; Strakhova, M.; Cowart, M. D.; Brioni, J. D. The histamine H3 receptor: an attractive target for the treatment of cognitive disorders. *Br. J. Pharmacol.* **2008**, 1–16. (f) Vohora, D.; Medhurst, A. D.; Carruthers, N. I.; Celanire, S.; Schwartz, J.-C.; Selbach, O.; Haas, H. L.; Panula, P.; Jin, C. Y.; Karlstedt, K.; Bakker, R.; Lebon, F.; Stark, H.; Coruzzi, G.; Adami, M.; Passani, M.; Blandina, P.; Brownan, K. E.; Fox, G. B.; Shelton, J. E.; Lovenberg, T. W.; Dugovc, C.; Esbenshade, T. A.; Brune, M. E.; Strakhova, M. I.; Pillai, K.; Browman, K. E.; Zhang, M.; Rueter, L. E.; Chazot, P.; Shenton, F. C. In *The Third Histamine Receptor*; Vohora, D., Eds.; CRC Press: Boca Raton, FL, 2009.

(17) Wieland, K.; Bongers, G.; Yamamoto, Y.; Hashimoto, T.; Yamatodani, A.; Menge, W. M. B. P.; Timmerman, H.; Lovenberg, T. W.; Leurs, R. Constitutive activity of histamine H3 receptors stably expressed in SK-N-MC cells: display of agonism and inverse agonism by H3 antagonists. *J. Pharm. Exp. Ther.* **2001**, *299*, 908–914.

(18) (a) Esbenshade, T. A.; Krueger, K. M.; Yao, B. B.; Witte, D. G.; Estvander, B. R.; Baranowski, J. L.; Miller, T. R.; Hancock, A. A. Differences in Pharmacological Properties of Histamine H(3) Receptor Agonists and Antagonists Revealed at Two Human H(3) Receptor Isoforms. Presented at the European Histamine Research Society Congress, 2006; Poster. (b) Bakker, R. A.; Lozada, A. F.; van Marle, A.; Shenton, F. C.; Drutel, G.; Karlstedt, K.; Hoffmann, M.; Lintunen, M.; Yamamoto, Y.; van Rijn, R. M.; Chazot, P. L.; Panula, P.; Leurs, R. Discovery of naturally occurring splice variants of the rat histamine H3 receptor that act as dominant-negative isoforms. *Mol. Pharmacol.* **2006**, *69*, 1194–1206. (c) Strakhova, M. I.; Fox, G. F.; Carr, T. L.; Witte, D. G.; Vortherms, T. A.; Manelli, A. M.; Miller, T. R.; Yao, B. B;; Brioni, J. D.; Esbenshade, T. A. Cloning and characterization of the monkey histamine H3 receptor isoforms. *Eur. J. Pharmacol.* **2008**, *601*, 8–15.

(19) (a) Barbier, A. J.; Bradbury, M. J. Histaminergic control of sleep−wake cycles: recent therapeutic advances for sleep and wake disorders. *CNS Neurol. Disord.: Drug Targets* **2007**, *6*, 31–43. (b) Passani, M. B.; Lin, J.-S.; Hancock, A.; Crochet, S.; Blandina, P. The histamine H3 receptor as a novel therapeutic target for cognitive and sleep disorders. *Trends Pharmacol. Sci.* **2004**, *25*, 618–625. (c) Parmentier, R.; Anaclet, C.; Guhennec, C.; Brousseau, E.; Bricout, D.; Giboulot, T.; Bozyczko-Coyne, D.; Spiegel, K.; Ohtsu, H.; Williamns, M.; Lin, J.-S. The brain H3-receptor as a novel therapeutic target for vigilance and sleep−wake disorders. *Biochem. Pharmacol.* **2007**, *73*, 1157–1171.

(20) (a) Hancock, A. A.; Brune, M. E. Assessment of pharmacology and potential anti-obesity properties of H3 receptor antagonists/inverse agonists. *Expert Opin. Invest. Drugs* **2005**, *14*, 223–241. (b) Malmlof, K.; Hohlweg, R.; Rimvall, K. Targeting of the central histaminergic system for treatment of obesity and associated metabolic disorders. *Drug Dev. Res.* **2006**, *67*, 651–665.

(21) Stark, H.; Sippl, W.; Ligneau, X.; Arrang, J.-M.; Ganellin, C. R.; Schwartz, J.-C.; Schunack, W. Different antagonist binding properties of human and rat histamine H3 receptors. *Bioorg. Med. Chem. Lett.* **2001**, *11*, 951–954.

(22) Yang, R.; Hey, J. A.; Aslanian, R.; Rizzo, C. A. Coordination of histamine H3 receptor antagonists with human adrenal cytochrome P450 enzymes. *Pharmacology* **2002**, *66*, 128–135.

(23) Hancock, A. A. The challenge of drug discovery of a GPCR target: analysis of preclinical pharmacology of histamine H3 antagonists/inverse agonists. *Biochem. Pharmacol.* **2006**, *71*, 1103–1113.

(24) Barbier, A. J.; Berridge, C.; Dugovic, C.; Laposky, A. D.; Wilson, S. J.; Boggs, J.; Aluisio, L.; Lord, B.; Mazur, C.; Pudiak, C. M.; Langlois, X.; Xiao, W.; Apodaca, R.; Carruthers, N. I.; Lovenberg, T. W. Acute wake-promoting actions of JNJ-5207852, a novel, diamine-based H3 antagonist. *Br. J. Pharmacol.* **2004**, *143*, 649–661.

(25) Hancock, A. A.; Bennani, Y. L.; Bush, E. N.; Esbenshade, T. A.; Faghih, R.; Fox, G. B.; Jacobson, P.; Knourek-Segel, V.; Krueger, K. M.; Nuss, M. E.; Pan, J. B.; Shapiro, R.; Witte, D. G.; Yao, B. B. Antiobesity effects of A-331440, a novel non-imidazole histamine H3 receptor antagonist. *Eur. J. Pharmacol.* **2004**, *487*, 183–197.

(26) Hancock, A. A.; Bitner, R. S.; Krueger, K. M.; Otte, S.; Nikkel, A. L.; Fey, T. A.; Bush, E. N.; Dickinson, R. W.; Shapiro, R.; Knourek-Segel, V.; Droz, B. A.; Brune, M. E.; Jacobson, P. B.; Cowart, M. D.; Esbenshade, T. A. Distinctions and contradistinctions between anti-obesity histamine H3 receptor (H3R) antagonists compared to cognition-enhancing H3 receptor antagonists. *Inflammation Res.* **2006**, *55*, S42−S44.

(27) Hancock, A. A.; Diehl, M. S.; Faghih, R.; Bush, E. N.; Krueger, K. M.; Krishna, G.; Miller, T. R.; Wilcox, D. M.; Nguyen, P.; Pratt, J. K.;

Cowart, M. D.; Eshenshade, T. A.; Jacobson, P. B. In vitro optimization of structure activity relationships of analogs of A-331440 combining radioligand receptor binding assays and micronucleus assays of potential antiobesity histamine H3 receptor antagonists. *Basic Clin. Pharmacol. Toxicol*. **2004**, *95*, 144–152.

(28) Esbenshade, T. A.; Fox, G. B.; Krueger, K. M.; Baranowski, J. L.; Miller, T. R.; Kang, C. H.; Denny, L. I.; Witte, D. G.; Yao, B. B.; Pan, J. B.; Faghih, R.; Bennani, Y. L.; Williams, M.; Hancock, A. A. Pharmacological and behavioral properties of A- 349821, a selective and potent human histamine H3 receptor antagonist. *Biochem. Pharmacol*. **2004**, *68*, 933–945.

(29) (a) Cowart, M.; Faghih, R.; Curtis, M. P.; Gfesser, G. A.; Bennani, Y. L.; Black, L. A.; Pan, L.; Marsh, K. C.; Sullivan, J. P.; Esbenshade, T. A.; Fox, G. B.; Hancock, A. A. 4-(2-[2-(2(*R*)-Methylpyrrolidin-1-yl)ethyl]benzofuran-5-yl)benzonitrile and related 2-aminoethylbenzofuran H3 receptor antagonists potently enhance cognition and attention. *J. Med. Chem.* **2005**, *48*, 38–55. (b) Esbenshade, T. A.; Fox, G. B.; Krueger, K. M.; Miller, T. R.; Kang, C. H.; Denny, L. I.; Witte, D. G.; Yao, B. B.; Pan, L.; Wetter, J.; Marsh, K.; Bennani, Y. L.; Cowart, M. D.; Sullivan, J. P.; Hancock, A. A. Pharmacological properties of ABT-239 [4-(2-{2-[(2*R*)-2-methylpyrrolidinyl]ethyl}-benzofuran-5-yl)benzonitrile]: I. Potent and selective histamine H3 receptor antagonist with drug-like properties. *J. Pharmacol. Exp. Ther*. **2005**, *313*, 165–175. (c) Fox, G. B.; Esbenshade, T. A.; Pan, J. B.; Radek, R. J.; Krueger, K. M.; Yao, B. B.; Browman, K. E.; Buckley, M. J.; Ballard, M. E.; Komater, V. A.; Miner, H.; Zhang, M.; Faghih, R.; Rueter, L. E.; Scott Bitner, R.; Drescher, K. U.; Wetter, J.; Marsh, K.; Lemaire, M.; Porsolt, R. D.; Bennani, Y. L.; Sullivan, J. P.; Cowart, M. D.; Decker, M. W.; Hancock, A. A. Pharmacological properties of ABT-239 [4-(2-{2-[(2*R*)-2-methylpyrrolidinyl]ethyl}-benzofuran-5-yl)benzonitrile]: II. Neurophysiological characterization and broad preclinical efficacy in cognition and schizophrenia of a potent and selective histamine H3 receptor antagonist. *J. Pharmacol. Exp. Ther*. **2005**, *313*, 176–190.

(30) Black, L. A.; Liu, H.; Diaz, G. J.; Fox, G. B.; Browman, K. E.; Wetter, J.; Marsh, K. C.; Miller, T. R.; Esbenshade, T. A.; Brioni, J.; Cowart, M. D. Minimization of potential hERG liability in histamine H3 receptor antagonists. *Inflammation Res*. **2008**, *57*, S45–S46.

(31) Malmloef, K.; Hastrup, S.; Schellerup Wulff, B.; Hansen, B. C.; Peschke, B.; Bekker Jeppesen, C.; Hohlweg, R.; Rimvall, K. Antagonistic targeting of the histamine H3 receptor decreases caloric intake in higher mammalian species. *Biochem. Pharmacol*. **2007**, *73*, 1237–1242.

(32) Ligneau, X.; Perrin, D.; Landais, L.; Camelin, J.-C.; Calmels, T. P. G.; Berrebi-Bertrand, I.; Lecomte, J.-M.; Parmentier, R.; Anaclet, C.; Lin, J.-S.; Bertaina-Anglade, V.; Drieu la Rochelle, C.; d'Aniello, F.; Rouleau, A.; Gbahou, F.; Arrang, J.-M.; Ganellin, C. R.; Stark, H.; Schunack, W.; Schwartz, J.-C. BF2.649 [1-{3-[3-(4-Chlorophenyl)propoxy]propyl}piperidine, hydrochloride], a non-imidazole inverse agonist/antagonist at the human histamine H3 receptor: preclinical pharmacology. *J. Pharmacol. Exp. Ther*. **2006**, *320*, 365–375.

(33) Medhurst, A. D.; Atkins, A. R.; Beresford, I. J.; Brackenborough, K.; Briggs, M. A.; Calver, A. R.; Cilia, J.; Cluderay, J. E.; Crook, B.; Davis, J. B.; Davis, R. K.; Davis, R. P.; Dawson, L. A.; Foley, A. G.; Gartlon, J.; Gonzalez, M. I.; Heslop, T.; Hirst, W. D.; Jennings, C.; Jones, D. N. C.; Lacroix, L. P.; Martyn, A.; Ociepka, S.; Ray, A.; Regan, C. M.; Roberts, J. C.; Schogger, J.; Southam, E.; Stean, T. O.; Trail, B. K.; Upton, N.; Wadsworth, G.; Wald, J. A.; White, T.; Witherington, J.; Woolley, M. L.; Worby, A.; Wilson, D. M. GSK189254, a novel H3 receptor antagonist that binds to histamine H3 receptors in Alzheimer's disease brain and improves cognitive performance in preclinical models. *J. Pharmacol. Exp. Ther*. **2007**, *321*, 1032–1045.

(34) Obecure Press Release. August 30, 2007. http://www.obecure.com.

(35) Fossati, A.; Barone, D.; Benvenuti, C. Binding affinity profile of betahistine and its metabolites for central histamine receptors of rodents. *Pharmacol. Res*. **2001**, *43*, 389–392.

(36) Reviews: (a) Celanire, S.; Wijtmans, M.; Talaga, P.; Leurs, P.; de Esch, I. J. P. Histamine H3 receptor antagonists reach out for the clinic. *Drug Discovery Today* **2005**, *10*, 1613. (b) Sander, K.; Kottke, T.; Stark, H. Histamine H_3 receptor antagonists go to clinics. *Biol. Pharm. Bull*. **2008**, *31*, 2163–2181.

(37) Kuttab, S.; Kalgutkar, A.; Castagnoli, N. Mechanistic studies on the monoamine oxidase B catalyzed oxidation of 1,4-disubstituted tetrahydropyridines. *Chem. Res. Toxicol*. **1994**, *7*, 740–744.

(38) Wilchek, M.; Spande, T. F.; Witkop, B.; Milne, G. W. A. Chemical conversion of tyrosine to 6-hydroxyindoles. *J. Am. Chem. Soc*. **1967**, *89*, 3349–3350.

(39) Cruz-Lopez, O.; Diaz-Mochon, J. J.; Campos, J. M.; Entrena, A.; Nunez, M. T.; Labeaga, L.; Orjales, A.; Gallo, M. A.; Espinosa, A. Design, syntheses, biological evaluation, and docking studies of 2-substituted 5-methylsulfonyl-1-phenyl-1*H*-indoles: potent and selective in vitro cyclooxygenase-2 inhibitors. *ChemMedChem* **2007**, *2*, 88–100, and references cited therein.

(40) Zaragoza, F.; Stephensen, H.; Knudsen, S. M.; Pridal, L.; Wulff, B. S.; Rimvall, K. 1-Alkyl-4-acylpiperazines as a new class of imidazole-free histamine H3 receptor antagonists. *J. Med. Chem*. **2004**, *47*, 2833–2838.

(41) Lindwall, H. G.; Mantell, G. J. Synthesis and reactions of indole carboxylic acids; pyridindolones from indole-2-carboxyacetalylbenzylamides. *J. Org. Chem*. **1953**, *18*, 345–357.

(42) Bashford, K. E.; Cooper, A. L.; Kane, P. D.; Moody, C. J.; Muthusamy, S.; Swann, E. N−H insertion reactions of rhodium carbenoids. Part 3. The development of a modified Bischler indole synthesis and a new protecting-group strategy for indoles. *J. Chem. Soc., Perkin Trans. 1* **2002**, 1672–1687.

(43) Roche, O.; Rodriguez Sarmiento, R. M. A new class of histamine H3 receptor antagonists derived from ligand based design. *Bioorg. Med. Chem. Lett*. **2007**, *17*, 3670–3675.

(44) Roche, O.; Nettekoven, M.; Vifian, W.; Rodriguez Sarmiento, R. M. Refinement of histamine H3 ligands pharmacophore model leads to a new class of potent and selective naphthalene inverse agonists. *Bioorg. Med. Chem. Lett*. **2008**, *18*, 4377–4379.

(45) Nettekoven, M.; Plancher, J.-M.; Richter, H.; Roche, O.; Rodriguez Sarmiento, R. M.; Taylor, S. Selective naphtalene H3 receptor inverse agonists with reduced potential to induce phospholipidosis and their quinoline analogs. *Bioorg. Med. Chem. Lett.*, in press.

(46) The amphiphilicity is the vector sum calculated from the charged group to each atom/residue within a molecule and weighted with respect to its hydrophobic/hydrophilic property on the basis of an atom/fragment based contribution method. The sum of the calculated vectors is calibrated by means of measured amphiphilicities, taking into account the conformational effects of the individual molecules. For a more detail description, see the following: (a) Fischer, H.; Kansy, M.; Bur, D. CAFCA: a novel tool for the calculation of amphiphilic properties of charged drug molecules. *Chimia* **2000**, *54*, 640. (b) Fischer, H.; Kansy, M.; Potthast, M.; Csato, M. *Proceedings of the 13th European Symposium on Quantitative Structure−Activity Relationships*, Düsseldorf, Germany, Aug 27−Sep 1, 2000; Prous Science: Barcelona, Spain, 2001.

(47) (a) Fox, G. B.; Pan, J. B.; Esbenshade, T. A.; Bitner, R. S.; Nikkel, A. L.; Miller, T.; Kang, C. H.; Bennani, Y. L.; Black, L. A.; Faghih, R.; Hancock, A. A.; Decker, M. W. Differential in vivo effects of H3 receptor ligands in a new mouse dipsogenia model. *Pharmacol., Biochem. Behav*. **2002**, *72*, 741–750. (b) Ligneau, X.; Lin, J.-S.; Vanni-Mercier, G.; Jouvet, M.; Muir, J. L.; Ganellin, C. R.; Stark, H.; Elz, S.; Schunack, W.; Schwartz, J.-C. Neurochemical and behavioral effects of ciproxifan, a potent histamine H3-receptor antagonist. *J. Pharmacol. Exp. Ther*. **1998**, *287*, 658–666.

(48) H_3R is potentially involved in a wide range of CNS side effects that could have an impact on the safety of the future drug and could also bias the assessment of efficacy, particularly in obesity models (e.g., sedation has an obvious but undesired effect on food intake). In order to gauge early the risk of CNS-mediated side effects, the first in vivo safety assay was incorporated into our screening cascade prior to testing of any in vivo efficacy models. The CNS-mediated side effects assay is based on visual inspection adapted from the IRWIN assay and run at a fixed dose of 30 mg/kg ip of test compound. Irwin, S. Comprehensive observational assessment: la. A systematic quantitative procedure for assessing the behavioural and physiologic state of the mouse. *Psychopharmacology* **1968**, *13*, 222–257.

(49) (a) Jia, L.; Sun, H. Support vector machines classification of hERG liabilities based on atom types. *Bioorg. Med. Chem*. **2008**, *16*, 6252–6260. (b) Raschi, E.; Vasina, V.; Poluzzi, E.; De Ponti, F. The hERG K+ channel: target and antitarget strategies in drug development. *Pharmacol. Res*. **2008**, *57*, 181–195. (c) Waring, M. J.; Johnstone, C. A quantitative assessment of hERG liability as a function of lipophilicity. *Bioorg. Med. Chem. Lett*. **2007**, *17*, 1759–1764. (d) Aronov, A. M. Common pharmacophores for uncharged human ether-a-go-go-related gene (hERG) blockers. *J. Med. Chem*. **2006**, *49*, 6917–6921.

(50) Fischer, H.; Kansy, M. Automated Generation of Multi-Dimensional Structure Activity and Structure Property Relationships. PCT Int. Appl. US 2007027632 A1, 2007.

(51) Kansy, M.; Senner, F.; Gubernator, K. Physicochemical high throughput screening: parallel artificial membrane permeation assay in the description of passive absorption processes. *J. Med. Chem*. **1998**, *41*, 1007–1010.

(52) Malmlof, K.; Zaragoza, F.; Golozoubova, V.; Refsgaard, H. H. F.; Cremers, T.; Raun, K.; Wulff, B. S.; Johansen, P. B.; Westerink, B.; Rimvall, K. Influence of a selective histamine H3 receptor antagonist on hypothalamic neural activity, food intake and body weight. *Int. J. Obes*. **2005**, *29*, 1402–1412.

(53) (a) Nettekoven, M.; Plancher, J.-M.; Richter, H.; Roche, O.; Taylor, S. Preparation of Substituted 5-(Aminocarbonyl)indole-2-carboxamides

as Histamine H3 Receptor Modulators for Treatment of Obesity, Diabetes and Dyslipidemia. PCT Int. Appl. WO 2007115938A1, 2007. (b) Nettekoven, M.; Plancher, J.-M.; Roche, O.; Takahashi, T.; Taylor, S. Preparation of Aminocyclohexyl Piperazinyl Methanones as Histamine H3 Receptor Modulators. PCT Int. Appl. WO 2007080140, 2007. (c) Nettekoven, M.; Plancher, J.-M.; Richter, H.; Roche, O.; Taylor, S. Preparation of Heterocyclic Indolecarboxamides as Histamine H3 Receptor Antagonists. U.S. Pat. Appl. Publ. US 2007123525 A1, 2007. (d) Nettekoven, M.; Plancher, J.-M.; Richter, H.; Roche, O.; Rodriguez Sarmiento, R. M.; Taylor, S. Preparation of 1,1-Dioxothiomorpholinyl Indolyl Methanone Derivatives as Histamine H3 Receptor Modulators for the Treatment of Obesity and Diabetes. U.S. Pat. Appl. Publ. US 2007123526 A1, 2007. (e) Nettekoven, M.; Plancher, J.-M.; Richter, H.; Roche, O.; Runtz-Schmitt, V.; Taylor, S. Preparation of Indole-2-carboxamides as Histamine H3 Receptor Modulators for the Treatment of Diabetes. U.S. Pat. Appl. Publ. US 2007123515 A1, 2007. (f) Nettekoven, M.; Plancher, J.-M.; Richter, H.; Roche, O.; Taylor, S. Preparation of Azaindole-2-carboxamides as Histamine H3 Receptor Modulators for the Treatment of Obesity, Diabetes and Dyslipidemia. PCT Int. Appl. WO 2007057329 A1, 2007. (g) Nettekoven, M. H.; Plancher, J.-M.; Roche, O.; Rodriguez-Sarmiento, R. M. Preparation of 5-Aminoindole Derivatives for Use as H3 Inverse Agonists. U.S. Pat. Appl. Publ. US 2006160855 A1, 2006.

JM900409X